


## Article

# Poisoning and Reuse of Supported Precious Metal Catalysts in the Hydrogenation of *N*-Heterocycles, Part II: Hydrogenation of 1-Methylpyrrole over Rhodium

László Hegedűs <sup>1,\*</sup> , Tien Thuy Thanh Nguyen <sup>1</sup> , Krisztina Lévy <sup>1</sup>, Krisztina László <sup>2</sup> , György Sáfrán <sup>3</sup> and Andrea Beck <sup>4</sup>

<sup>1</sup> Department of Organic Chemistry and Technology, Faculty of Chemical Technology and Biotechnology, Budapest University of Technology and Economics, Műgyetem rkp. 3, H-1111 Budapest, Hungary; thuytien.nguyenthanh@edu.bme.hu (T.T.T.N.); levaykrisztina@edu.bme.hu (K.L.)

<sup>2</sup> Department of Physical Chemistry and Materials Science, Faculty of Chemical Technology and Biotechnology, Budapest University of Technology and Economics, Műgyetem rkp. 3, H-1111 Budapest, Hungary; laszlo.krisztina@vbk.bme.hu

<sup>3</sup> Thin Film Physics Department, Institute for Technical Physics and Materials Science, Centre for Energy Research, Eötvös Loránd Research Network (ELKH), Konkoly-Thege Miklós út 29–33, H-1121 Budapest, Hungary; safran.gyorgy@ek-cer.hu

<sup>4</sup> Surface Chemistry and Catalysis Department, Institute for Energy Security and Environmental Safety, Centre for Energy Research, Eötvös Loránd Research Network (ELKH), Konkoly-Thege Miklós út 29–33, H-1121 Budapest, Hungary; beck.andrea@ek-cer.hu

\* Correspondence: hegedus.laszlo@vbk.bme.hu; Tel.: +36-1-4631261



**Citation:** Hegedűs, L.; Nguyen, T.T.T.; Lévy, K.; László, K.; Sáfrán, G.; Beck, A. Poisoning and Reuse of Supported Precious Metal Catalysts in the Hydrogenation of *N*-Heterocycles, Part II: Hydrogenation of 1-Methylpyrrole over Rhodium. *Catalysts* **2022**, *12*, 730. <https://doi.org/10.3390/catal12070730>

Academic Editors: Antal Csampa, Tamás Jernei and Victorio Cadierno

Received: 17 May 2022

Accepted: 29 June 2022

Published: 1 July 2022

**Publisher's Note:** MDPI stays neutral with regard to jurisdictional claims in published maps and institutional affiliations.



**Copyright:** © 2022 by the authors. Licensee MDPI, Basel, Switzerland. This article is an open access article distributed under the terms and conditions of the Creative Commons Attribution (CC BY) license (<https://creativecommons.org/licenses/by/4.0/>).

**Abstract:** Poisoning effect of nitrogen on heterogeneous, supported precious metal catalysts, along with their recycling, was further examined in the liquid-phase hydrogenation of 1-methylpyrrole (MP) to 1-methylpyrrolidine (MPD) over rhodium on carbon or  $\gamma$ -alumina, in methanol, under non-acidic conditions, at 25–50 °C and 10 bar. Reusing a spent, unregenerated 5% Rh/C or 5% Rh/ $\gamma$ -Al<sub>2</sub>O<sub>3</sub> catalyst, it was found that the conversion of this model substrate and the activity of the catalyst were strongly dependent on the amount of catalyst, the type of support, the catalyst pre- or after-treatment, the temperature, and the number of recycling, respectively. An unexpected catalytic behaviour of rhodium was observed when it was used in a prehydrogenated form, because no complete conversion of MP was achieved over even the fresh Rh/C or Rh/ $\gamma$ -Al<sub>2</sub>O<sub>3</sub>, contrary to the untreated one. In addition, there was a significant difference in the reusability and activity of these rhodium catalysts, depending on their supports (activated carbon,  $\gamma$ -alumina). These diversions were elucidated by applying dispersion (O<sub>2</sub>- and H<sub>2</sub>-titration), temperature-programmed desorption of ammonia (NH<sub>3</sub>-TPD), and transmission electron microscopy (TEM) measurements.

**Keywords:** hydrogenation; poisoning; reusing; rhodium; pyrroles; pyrrolidines; spent catalyst

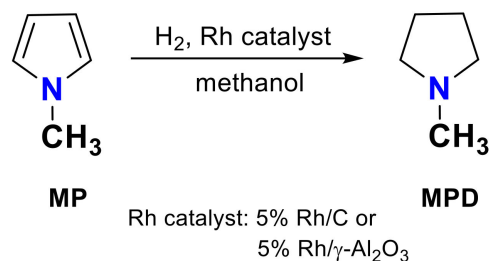
## 1. Introduction

In our previous study [1], the heterogeneous catalytic hydrogenation of 1-methylpyrrole (MP) to 1-methylpyrrolidine (MPD) over ruthenium, in methanol (a non-acidic medium), at 25–60 °C and 10 bar, was reported, and the poisoning phenomena of a 5% Ru/C catalyst provoked by nitrogen and its reusability in an unregenerated form were elucidated.

As well-known [2–9], several types of catalyst deactivation (fouling, poisoning, thermal degradation, vapour–solid and/or solid–solid reactions, attrition/crushing) can be responsible for decreasing or ceasing the activity of catalysts, among which poisoning is a strong chemisorption of different species (products, reactants, or impurities) on the catalytically active centres blocking the surface chemical reactions. It has also long been known [10–22] that nitrogen-containing compounds have inhibitory influences on the hydrogenation catalysts due to their non-bonding electron pairs. This effect can be eliminated

by conversion of these substances to a form in which the N atom is protected—for example, by adding protic acids (e.g.,  $\text{H}_2\text{SO}_4$ ,  $\text{HCl}$ ) [12]. Nevertheless, this method cannot be applied if side reactions (e.g., polymerisation) take place under acidic conditions, as was observed during the reduction of a pyrrole derivative (1-methyl-2-pyrroleethanol) [23,24].

In this work, continuing our systematic investigations in this research area, the poisoning phenomena of heterogeneous, supported precious metal catalysts caused by nitrogen, and their reuse without regeneration, were examined in detail. Based on our previous experience [25], the liquid-phase hydrogenation of 1-methylpyrrole (MP) to 1-methylpyrrolidine (MPD) over 5% rhodium on carbon or  $\gamma$ -alumina, in a non-acidic medium (methanol), was also chosen as a model reaction (Scheme 1).



**Scheme 1.** Rhodium-catalysed hydrogenation of 1-methylpyrrole (MP) to 1-methylpyrrolidine (MPD) under non-acidic conditions.

Pyrrolidines are important and valuable pharmaceutical intermediates [23–30], such as 1-methyl-2-pyrrolidineethanol [23,24] applied for the synthesis of clemastine [27–29] or methyl 1-methyl-2-pyrrolidineacetate [26] used for the biosynthesis of cocaine [30]. During our previous investigations [23–26], it was found that the light platinum metals (Rh, Ru, Pd) proved to be the most active catalysts in the saturation of pyrrole ring. These hydrogenations took place smoothly under mild reaction conditions (25–80 °C, 6 bar), with complete conversion and high selectivity, but poisoning of the catalysts was observed below certain catalyst/substrate ratios. These ratio limits ranged from 0.03 to 0.20 g g<sup>−1</sup>, and they were dependent on the nature of the substrates, catalytic metals, and solvents. In addition, the poison sensitivity of these precious metals related to nitrogen was also specified, which decreased in the following sequence: Pd > Ru >> Rh. This order was ascribed to electronic factors [31].

Rhodium is often used in the heterogeneous catalytic hydrogenation of pyrroles, typically in a supported form: on activated carbon [24–26,31–35], on alumina [24,25,34,36–42], or on silica [43]. For instance, 2,5-dimethylpyrrole was reduced to *cis*-2,5-dimethylpyrrolidine over 5% Rh/Al<sub>2</sub>O<sub>3</sub> (7% by weight of substrate) in acetic acid, at 3 bar and room temperature, with 70% yield [36]. During the diastereoselective saturation of the pyrrole ring under acid-free conditions, the rhodium-catalysed hydrogenation of *N*-(1'-methylpyrrole-2'-acetyl)-(S)-proline methyl ester resulted in the corresponding pyrrolidine derivative with complete conversion, 98% isolated yield, and 95% diastereomeric excess, in methanol, at 20 bar and 25 °C [32,33], while the reduction of ethyl 2-(3'-methoxy-1'-methyl-1'*H*-pyrrol-2'-yl)-2-oxoacetate over 5% Rh/Al<sub>2</sub>O<sub>3</sub>, in methanol, at 10 bar and 25 °C, gave one diastereomer of the product (a pyrrolidine derivative with three stereocentres) in 91% yield [39]. Using a Rh/C catalyst, pyrrole-2-carboxylic acid was converted to DL-proline with an excellent yield (98%), in isopropyl alcohol, at 30 bar and 100 °C [35]. Furthermore, dendrimer-encapsulated monodisperse Rh nanoparticles (~1 nm) immobilised onto a high-surface-area mesoporous silica support (SBA-15) were also applied in the hydrogenation of pyrrole to obtain pyrrolidine, applying 0.005 bar partial pyrrole and 0.5 bar partial H<sub>2</sub> pressures, at 60–100 °C. Both the Rh<sub>15</sub> and Rh<sub>30</sub> nanoparticles on SBA-15 showed similar activities, and pyrrolidine was formed with 100% selectivity after 3 h [40]. Recently, however, a Rh(111) single-crystal catalyst has also been applied in the vapour-phase reduction of pyrrole [44]. Nevertheless, to the best of our knowledge, no systematic investigations

concerning the poisoning and reusability of heterogeneous rhodium catalysts can be found in the literature.

In addition, handling the spent catalysts obtained after the hydrogenation reactions is also an important technological aspect of the heterogeneous catalytic processes in the chemical industry [45–55]. Both precious [45,46] and base [47] metals on different supports, or in pure metal or metal oxide forms, are usually fully regenerated before their reuse, but the applied regeneration methods (e.g., incineration or pyrometallurgical processes) are typically energy-intensive and expensive procedures. However, in the pharmaceutical industry, where precious metals on carbon catalysts (e.g., Pd/C, Rh/C) are widely used, the usual method is applying the completely regenerated spent catalysts, due to the very strict rules of quality assurance (*Good Manufacturing Practices—GMP* [56]). Their reuse without regeneration has not been solved thus far; therefore, an easy and less-expensive catalyst recycling process for the heterogeneous catalytic hydrogenations could allow the production of pharmaceuticals more economically.

In this paper, the effect of reusing the spent, unregenerated, carbon- or  $\gamma$ -alumina-supported rhodium (5% Rh/C, 5% Rh/ $\gamma$ -Al<sub>2</sub>O<sub>3</sub>) on their activities and conversion of **MP** is discussed. An unexpected behaviour of these catalysts was elucidated by dispersion (O<sub>2</sub>- and H<sub>2</sub>-titration) and temperature-programmed desorption of ammonia (NH<sub>3</sub>-TPD) surface characterisation methods.

## 2. Results and Discussion

### 2.1. Rhodium-Catalysed Reference Hydrogenations of 1-Methylpyrrole

Conversion of **MP** over 5% Rh/C and 5% Rh/ $\gamma$ -Al<sub>2</sub>O<sub>3</sub> catalysts, depending on the number of reusing the catalyst, at a 0.10 g · g<sup>−1</sup> catalyst/substrate ratio, in methanol, at 10 bar and 25 °C, is shown in Figure 1, while the initial rates ( $v_0$ ) and the reaction times in the hydrogenation of **MP** are summarised in Table 1.

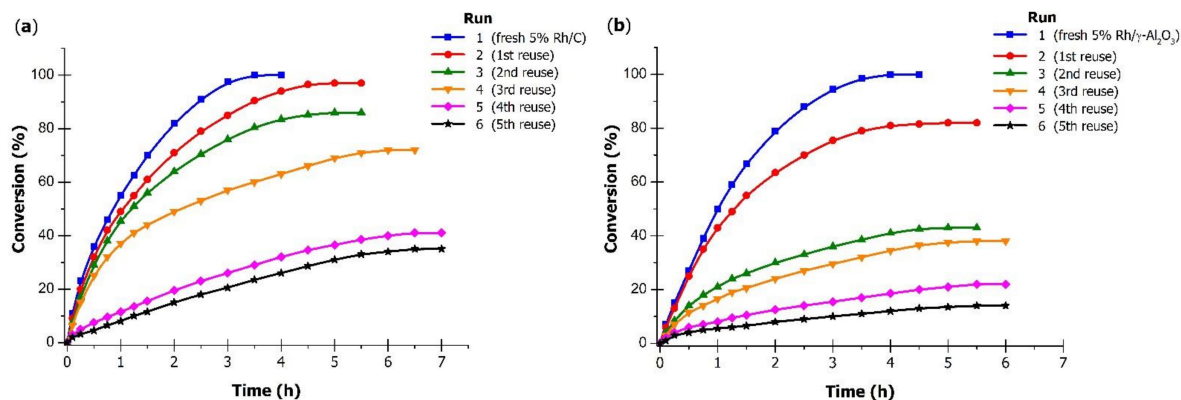


**Figure 1.** Reusing 5% Rh/C (a) or 5% Rh/ $\gamma$ -Al<sub>2</sub>O<sub>3</sub> (b) in the hydrogenation of 1-methylpyrrole (**MP**). Conditions: 2.0 g substrate, 0.2 g catalyst, 50 cm<sup>3</sup> methanol, 25 °C, 10 bar.

**Table 1.** Effects of reusing the catalyst (5% Rh/C or 5% Rh/ $\gamma$ -Al<sub>2</sub>O<sub>3</sub>) on the initial rate ( $v_0$ ) and the reaction time in the hydrogenation of 1-methylpyrrole (**MP**).

Run	Reusing the Catalyst	Reaction Time (h)		Conversion (%)		$v_0$ (nL H <sub>2</sub> · g <sub>Rh</sub> <sup>−1</sup> · h <sup>−1</sup> )	
		5% Rh/C	5% Rh/ $\gamma$ -Al <sub>2</sub> O <sub>3</sub>	5% Rh/C	5% Rh/ $\gamma$ -Al <sub>2</sub> O <sub>3</sub>	5% Rh/C	5% Rh/ $\gamma$ -Al <sub>2</sub> O <sub>3</sub>
1	— (Fresh)	3.5	4.0	100	100	121.8	77.5
2	1st	5.0	5.0	97	82	99.6	66.4
3	2nd	5.0	5.0	86	43	83.0	44.3
4	3rd	6.0	5.0	72	38	72.0	33.2
5	4th	6.5	5.5	41	22	33.2	22.2
6	5th	6.5	5.5	35	14	22.1	11.1

Conditions: 2.0 g substrate, 0.2 g catalyst, 50 cm<sup>3</sup> methanol, 25 °C, 10 bar.

As seen, both the fresh 5% rhodium on carbon and 5% rhodium on  $\gamma$ -alumina proved to be efficient catalysts for the hydrogenation of **MP**, because complete conversion was already obtained at 25 °C (Figure 1a,b, run 1), and only a slight difference could be observed in the reaction times: 3.5 h (5% Rh/C) and 4.0 h (5% Rh/ $\gamma$ -Al<sub>2</sub>O<sub>3</sub>). During the reuse of these catalysts, the saturation of pyrrole ring took place more slowly, and stopped at lower conversions than in the original reactions (Figure 1a,b, runs 2–6), contrary to the ruthenium-catalysed hydrogenation of **MP** [1], where full conversion was achieved in each repeated reduction at 10 bar and 25 °C.

However, there were differences in the course of hydrogenation of **MP** using these diverse supported rhodium catalysts. Although both the final conversions and the initial rates of the hydrogenation ( $v_0$ ) diminished constantly after each reuse of these catalysts (Table 1), a significant decrease was detected in the final conversion values (82 → 43%) after 5.0 h, between the first and second reuses of 5% Rh/ $\gamma$ -Al<sub>2</sub>O<sub>3</sub> (Figure 1b, runs 2 and 3), and the  $v_0$  values also decreased in a similar way (66.4 → 44.3 nL H<sub>2</sub> · g<sub>Rh</sub><sup>−1</sup> · h<sup>−1</sup>). Nevertheless, in case of 5% Rh/C, a similar appreciable diminution was observed in both the conversions (72 → 41%) and the initial rates (72.0 → 33.2 nL H<sub>2</sub> · g<sub>Rh</sub><sup>−1</sup> · h<sup>−1</sup>), but only after its third reuse (Figure 1a, runs 4 and 5). In the last recycling of these Rh catalysts (Figure 1a,b, run 6), low conversions (35% with 5% Rh/C and 14% with 5% Rh/ $\gamma$ -Al<sub>2</sub>O<sub>3</sub>, respectively) were achieved, indicating the strong poisoning of rhodium caused by basic nitrogen of the product (**MPD**), and these N-containing inhibitor molecules could not be removed from the surface of the catalysts at room temperature.

This lower poison tolerance of the 5% Rh/ $\gamma$ -Al<sub>2</sub>O<sub>3</sub> catalyst was presumably due to the more acidic character of the  $\gamma$ -alumina support [57]; thus, the very basic product (1-methylpyrrolidine) can adsorb more strongly and can accumulate in a higher amount on the surface of  $\gamma$ -Al<sub>2</sub>O<sub>3</sub> than on that of activated carbon with a neutral character. To confirm our hypothesis, temperature-programmed ammonia desorption (NH<sub>3</sub>-TPD) measurements were performed on both the fresh and used catalysts, as well as on their supports, as discussed in Section 2.3.

## 2.2. Effect of Temperature

Since these rhodium catalysts applied in this hydrogenation were strongly deactivated after their multiple (6×) uses and at 25 °C, the influence of higher temperatures (50 and 80 °C) on the conversion of **MP** over 5% rhodium on carbon or  $\gamma$ -alumina, and on the initial rate ( $v_0$ ), was also examined. Their dependence on the number of reusing the catalyst and the temperature, at a 0.1 g · g<sup>−1</sup> catalyst/substrate ratio, in methanol, at 10 bar, is depicted in Figures 2–5.

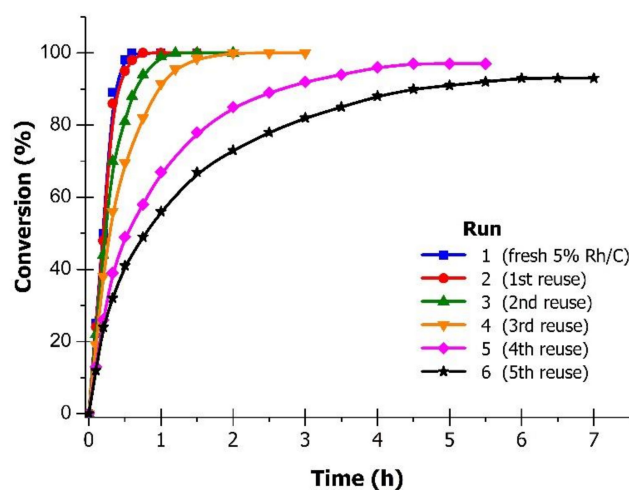


**Figure 2.** Conversion of 1-methylpyrrole (**MP**) vs. time over 5% Rh/C, at 50 °C. Conditions: 2.0 g substrate, 0.2 g catalyst, 50 cm<sup>3</sup> methanol, 10 bar.



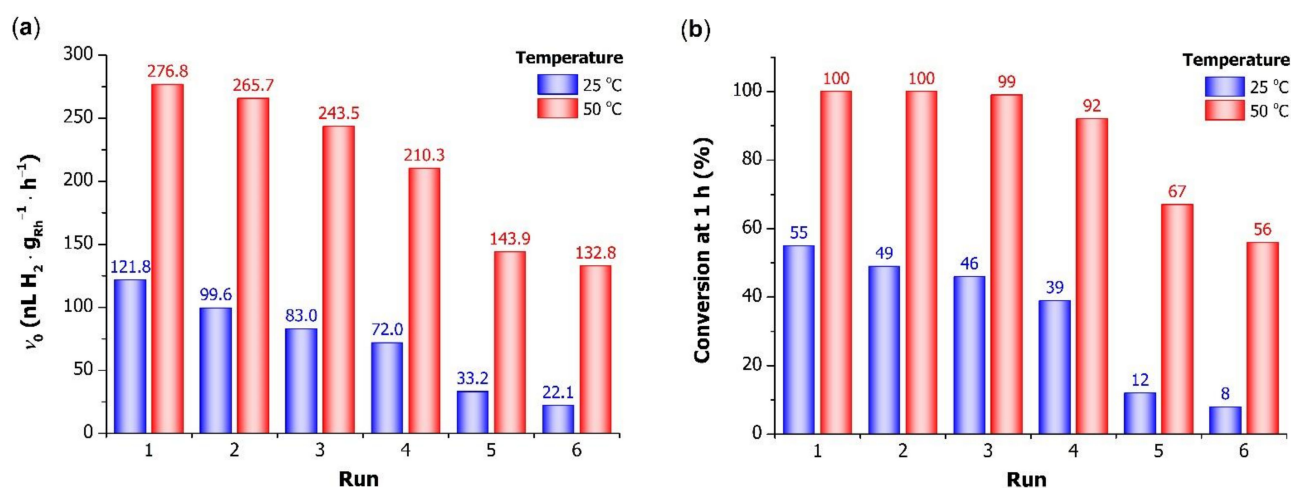


**Figure 3.** Effects of the temperature and reuse of the catalyst on the initial rate ( $v_0$ ) (a) and the conversion at 1 h (b) in the hydrogenation of 1-methylpyrrole (MP) over 5% Rh/C. Conditions: 2.0 g substrate, 0.2 g catalyst, 50 cm<sup>3</sup> methanol, 10 bar.

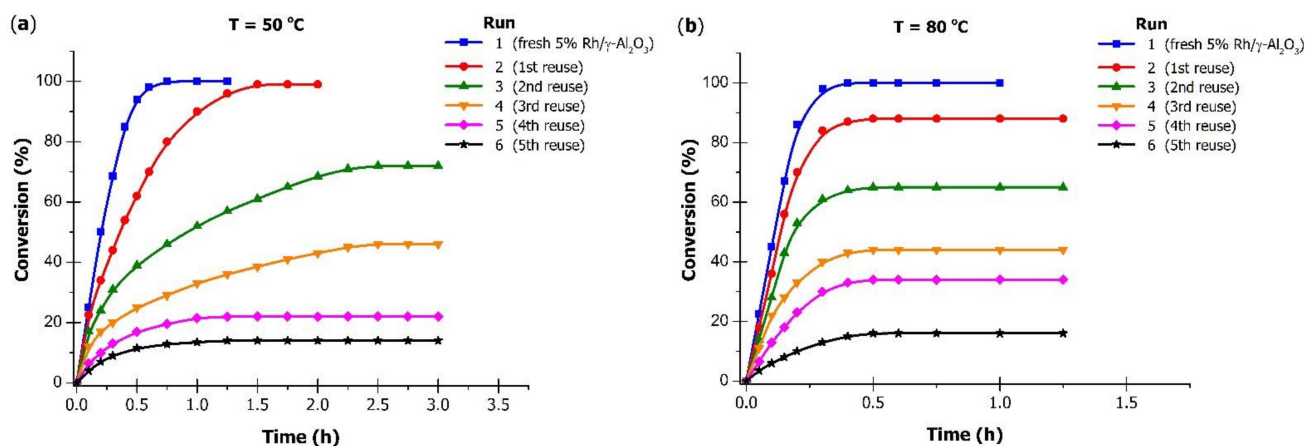


**Figure 4.** Conversion of 1-methylpyrrole (MP) vs. time over 5% Rh/ $\gamma$ -Al<sub>2</sub>O<sub>3</sub> at 50 °C (a) or 80 °C (b). Conditions: 2.0 g substrate, 0.2 g catalyst, 50 cm<sup>3</sup> methanol, 10 bar.

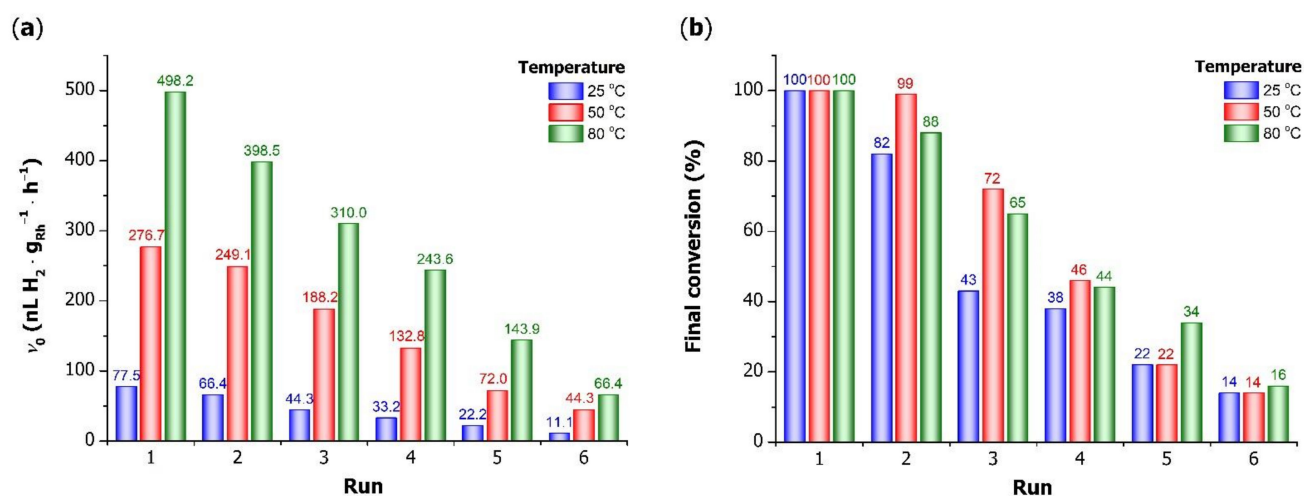


**Figure 5.** Influences of the temperature and reuse of the catalyst on the initial rate ( $v_0$ ) (a) and the final conversion (b) in the hydrogenation of 1-methylpyrrole (MP) over 5% Rh/ $\gamma$ -Al<sub>2</sub>O<sub>3</sub>. Conditions: 2.0 g substrate, 0.2 g catalyst, 50 cm<sup>3</sup> methanol, 10 bar.

At 50 °C, as shown in Figure 2, the hydrogenation of **MP** over the fresh 5% Rh/C was fast and complete within 0.6 h (run 1); moreover, the conversion was also 100% when applying the recycled catalyst until its third reuse (runs 2–4), but this required slightly longer reaction times (0.7 → 1.2 → 2.0 h). In the last two reactions (runs 5 and 6), the saturation of pyrrole ring was not complete even after 7 h, namely the H<sub>2</sub> uptake stopped at lower conversions (97 and 93%, respectively). Presumably, poisoning of the catalyst became more significant at this stage, and impeded the full conversion of **MP** even at 50 °C.

Comparing the results to those achieved at 25 °C, a notable increase was observed in both the initial rates and the 1 h conversions (Figure 3). As shown in Figure 3a, the  $v_0$  values were much higher at 50 °C (276.8–132.8 nL H<sub>2</sub> · g<sub>Rh</sub><sup>−1</sup> · h<sup>−1</sup>) than at 25 °C (121.8–22.1 nL H<sub>2</sub> · g<sub>Rh</sub><sup>−1</sup> · h<sup>−1</sup>), and a similar trend could be observed in the conversions obtained after 1 h at 50 °C (100 → 56%) and at 25 °C (55 → 8%) (Figure 3b). It seems, these inhibitor molecules (**MPD**) could more easily desorb from the surface of the catalyst at higher temperatures.

When 5% Rh/γ-Al<sub>2</sub>O<sub>3</sub> was applied at 50 °C (Figure 4a), similarly to the 5% Rh/C, the fresh catalyst was also able to saturate the pyrrole ring completely and quickly after 0.8 h (run 1). However, during its first reuse (run 2), only 99% conversion was obtained even within 2 h, and the hydrogen uptake ceased at this level. In the next two reuses (runs 3 and 4), the reduction of **MP** also stopped after 2.5 h, and the conversions became appreciably lower (72 and 46%, respectively). During the last two reactions (runs 5 and 6), the catalyst was completely deactivated already after 1 h, resulting in very weak conversion values (22 and 14%, respectively).

Further increasing the temperature to 80 °C (Figure 4b), the hydrogenation of **MP** over the fresh 5% rhodium on γ-alumina took place very quickly (0.5 h), with complete conversion (run 1). However, no complete saturation of the pyrrole ring was achieved even in the first reuse of the catalyst (run 2), namely the hydrogen uptake stopped at 88% conversion after 0.5 h. Similar behaviour of the used 5% Rh/γ-Al<sub>2</sub>O<sub>3</sub> could be observed during its all subsequent reuses (runs 3–6), resulting in a continuous decrease in the final conversions (65 → 16%).

Although applying the higher temperatures (50 and 80 °C) was accompanied by higher initial rates ( $v_0$ ), as shown in Figure 5a, the final conversions of **MP** were not significantly improved (Figure 5b), and the γ-alumina-supported rhodium catalyst was strongly poisoned after its fifth reuse (run 6). At the beginning of the hydrogenation, the higher temperature presumably favoured the desorption of inhibitory product molecules (**MPD**) from the surface of the catalyst, but later side reactions could take place (e.g., polymerisation of the pyrrole compound) due to the raised temperature and the more acidic character of γ-Al<sub>2</sub>O<sub>3</sub>, resulting in greater deactivation of the catalyst.

Comparing the results obtained by these different supported rhodium catalysts at 50 °C (Figure 6), it can be stated that 5% Rh/γ-Al<sub>2</sub>O<sub>3</sub> showed also lower poison tolerance than 5% Rh/C even at this higher temperature. The final conversions became much worse after the second reuse of the 5% Rh/γ-Al<sub>2</sub>O<sub>3</sub> catalyst (Figure 6b, run 3), while complete saturation of the pyrrole ring was obtained over 5% Rh/C in almost all cases (runs 1–4), and appreciably better final conversions were achieved (96 and 93%, respectively) in its last reuses (runs 5 and 6) than using 5% Rh/γ-Al<sub>2</sub>O<sub>3</sub> (22 and 14%, respectively).

According to these results, the increase of temperature from 25 to 50 °C resulted in higher catalyst activity and final conversions using 5% rhodium on carbon in all of its reuses, but in the case of 5% rhodium on γ-alumina, the raised temperature (50 or 80 °C) caused a significant conversion decrease and catalyst deactivation during its multiple reuses, i.e., the differences observed at 25 °C between these Rh catalysts on various supports became more remarkable at 50 °C.

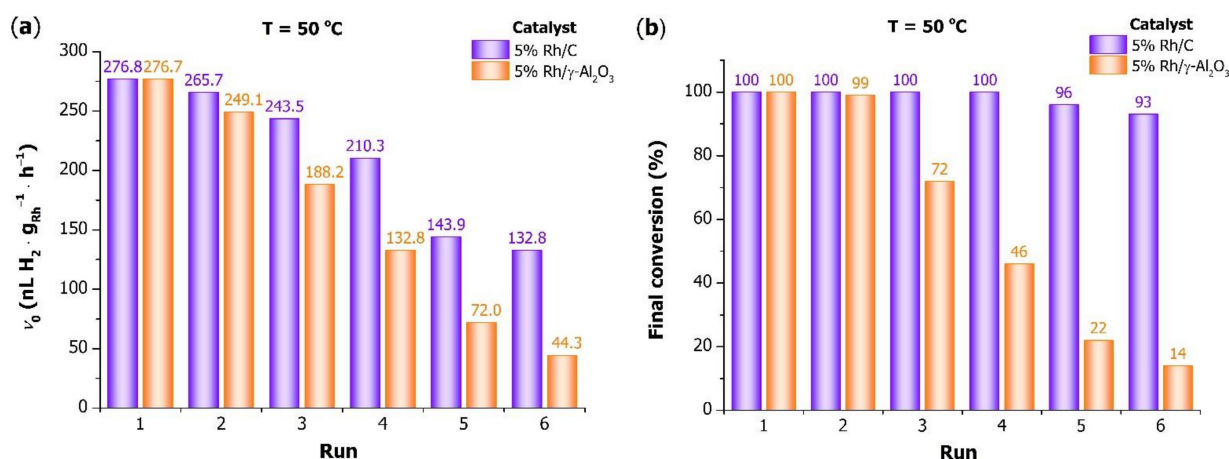


**Figure 6.** Effects of the supports (activated carbon,  $\gamma$ -alumina) and reuse of the catalyst on the initial rate ( $v_0$ ) (a) and the final conversion (b) in the Rh-catalysed hydrogenation of 1-methylpyrrole (MP), at  $50^\circ\text{C}$ . Conditions: 2.0 g substrate, 0.2 g catalyst,  $50\text{ cm}^3$  methanol,  $50^\circ\text{C}$ , 10 bar.

### 2.3. $\text{NH}_3$ -TPD Examinations

To explain the different behaviours observed previously (Sections 2.1 and 2.2), surface analytical investigations were performed using temperature-programmed ammonia desorption ( $\text{NH}_3$ -TPD) measurements to provide information about the surface acidity of the applied rhodium catalysts on different supports (activated carbon,  $\gamma$ -alumina).

The  $\text{NH}_3$ -TPD profiles of the fresh 5% Rh/C and 5% Rh/ $\gamma\text{-Al}_2\text{O}_3$  catalysts, as well as their supports, are shown in Figure 7. As seen in Figure 7a, both the 5% rhodium on carbon catalyst and its pure support show a characteristic  $\text{NH}_3$  desorption peak with a maximum at  $117^\circ\text{C}$ ; however, the peak of the pristine activated-carbon support has a tailing on the high-temperature side. This slight difference in the shape of the desorption peaks can indicate that the acidic centres on the surface of the activated carbon (e.g.,  $-\text{COOH}$  and  $-\text{OH}$  groups) are altered to a minimal extent during the deposition of rhodium metal particles. In case of the 5%  $\gamma$ -alumina-supported rhodium catalyst, two types of acid centres can be detected by the band with a maximum at  $120^\circ\text{C}$  and a shoulder at about  $251^\circ\text{C}$ . The strikingly lower-intensity broad characteristic  $\text{NH}_3$  desorption peak of pure  $\gamma\text{-Al}_2\text{O}_3$  has its maximum at the same temperature, but shows no clear higher-temperature shoulder. However, we cannot correlate these differences with the effect of Rh, since the two  $\gamma\text{-Al}_2\text{O}_3$  (the pure one and the other in Rh/ $\gamma\text{-Al}_2\text{O}_3$ ) are not the same.

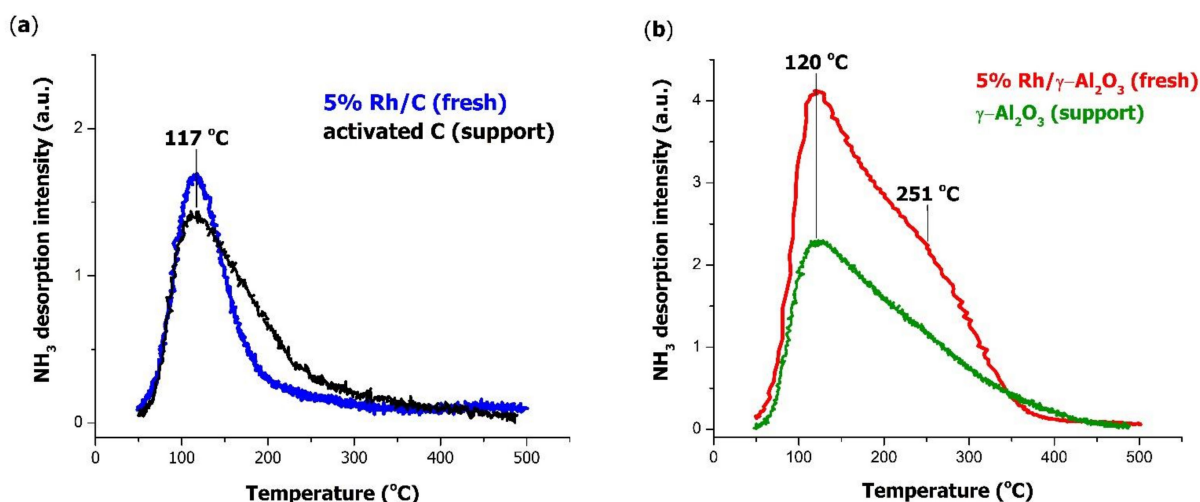


**Figure 7.**  $\text{NH}_3$ -TPD profiles of the fresh 5% Rh/C (a) and 5% Rh/ $\gamma\text{-Al}_2\text{O}_3$  (b) catalysts, as well as their supports (activated carbon,  $\gamma$ -alumina).

It should be noted that there was no opportunity to receive the  $\gamma$ -Al<sub>2</sub>O<sub>3</sub> support applied by the catalyst manufacturer; therefore, another, commercially available  $\gamma$ -alumina (Alfa Aesar) was purchased. To verify their similarities and/or differences, the BET surfaces ( $S_{\text{BET}}$ ) of both the catalysts and the supports were determined (Table 2). As seen, the specific surface area of the commercially available  $\gamma$ -Al<sub>2</sub>O<sub>3</sub> ( $135 \text{ m}^2 \cdot \text{g}^{-1}$ ) was approximately half that of the Degussa-type 5% Rh/ $\gamma$ -Al<sub>2</sub>O<sub>3</sub> catalyst ( $288 \text{ m}^2 \cdot \text{g}^{-1}$ ), while that of the activated carbon support (Carbopal P3) and 5% Rh/C catalyst were practically the same ( $940$  and  $880 \text{ m}^2 \cdot \text{g}^{-1}$ , respectively). The former explains the much lower intensity of the NH<sub>3</sub> desorption peak of  $\gamma$ -Al<sub>2</sub>O<sub>3</sub> compared to that of 5% Rh/ $\gamma$ -Al<sub>2</sub>O<sub>3</sub>.

**Table 2.** Characterisation data of the Rh catalysts and their supports.

Entry	Catalysts/Supports	$S_{\text{BET}}$ ( $\text{m}^2 \cdot \text{g}^{-1}$ )	NH <sub>3</sub> Desorption (norm. Peak Area $\cdot \text{g}_{\text{cat}}^{-1}$ )
1	$\gamma$ -Al <sub>2</sub> O <sub>3</sub> (Alfa Aesar)	135	23.9 *
2	5% Rh/ $\gamma$ -Al <sub>2</sub> O <sub>3</sub> , fresh (Degussa G214 R/D)	288	39.0
3	5% Rh/ $\gamma$ -Al <sub>2</sub> O <sub>3</sub> , used (Degussa G214 R/D)	n.m.	11.2
4	Activated C (Carbopal P3)	940	10.0
5	5% Rh/C, fresh (own-prepared)	880	8.8
6	5% Rh/C, used (own-prepared)	n.m.	5.2

norm. = normalised; n.m. = not measured. \*  $51.0 \text{ norm. peak area} / 288 \text{ m}^2$ .

The NH<sub>3</sub>-TPD profiles of the fresh and the 6× used 5% Rh/C and 5% Rh/ $\gamma$ -Al<sub>2</sub>O<sub>3</sub> catalysts applied in the reference hydrogenations (Section 2.1) are compared in Figure 8. It can be observed that the concentration of the acidic centres decreased significantly in the multiple used (6×) catalysts, both the carbon-supported (Figure 8a) and the  $\gamma$ -alumina-supported (Figure 8b) rhodium ones. In addition, in the used 5% Rh/ $\gamma$ -Al<sub>2</sub>O<sub>3</sub> catalyst, the shoulder at 251 °C, which indicates the stronger acidic sites, decreased to a higher extent. This could mean that the 1-methylpyrrolidine (MPD) was adsorbed on the acidic centres, and remained permanently on the surface of the catalyst (support).

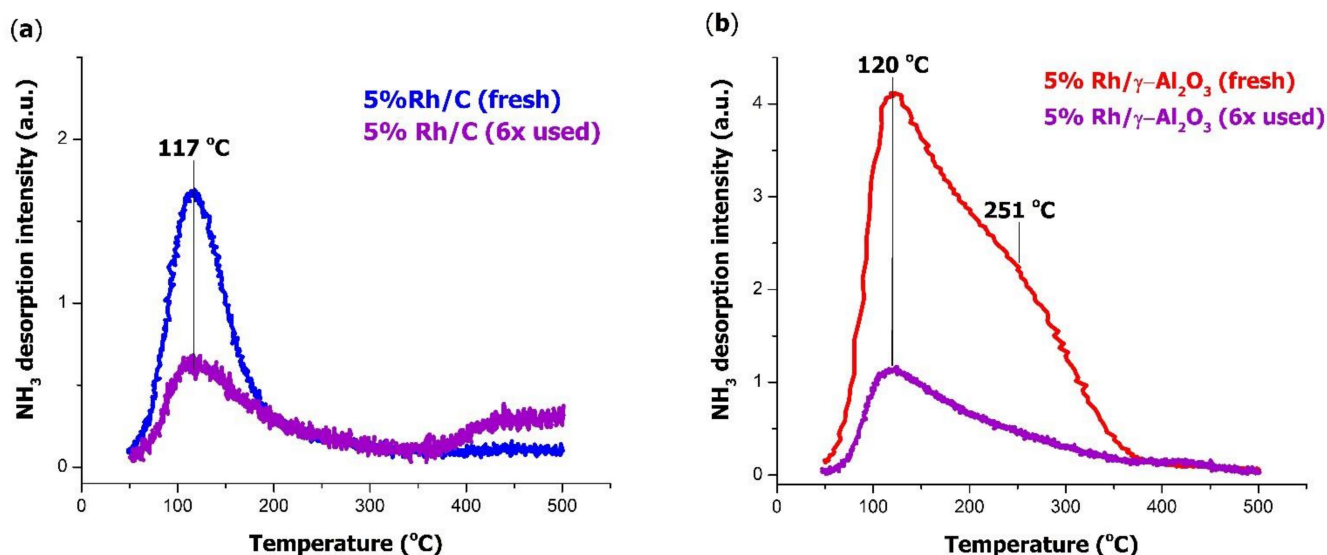


**Figure 8.** NH<sub>3</sub>-TPD profiles of the fresh and used (6×) 5% Rh/C (a) and 5% Rh/ $\gamma$ -Al<sub>2</sub>O<sub>3</sub> (b) catalysts.

Comparing the relative amounts of NH<sub>3</sub> desorbed from the different rhodium catalyst and their supports (Table 2), it is obvious that the  $\gamma$ -Al<sub>2</sub>O<sub>3</sub> support has much more acidic centres ( $23.9$  and  $39.0 \text{ norm. peak area} \cdot \text{g}_{\text{cat}}^{-1}$ ) than the activated-carbon one ( $10.0$  and  $8.8 \text{ norm. peak area} \cdot \text{g}_{\text{cat}}^{-1}$ ), which is consistent with the literature data [57]. Moreover, the density of acidic sites, i.e., their number on unit surface area, is even higher on the alumina surface, so they are much closer to each other on alumina than on carbon. However, it

can also be stated that the amount of surface acidic centres slightly diminished during the deposition of rhodium in case of both catalysts (39.0 and 8.8 norm. peak area·g<sub>cat</sub><sup>−1</sup>, respectively), taking into account the ca. twofold greater specific surface area of 5% Rh/γ-Al<sub>2</sub>O<sub>3</sub> compared to that of the γ-Al<sub>2</sub>O<sub>3</sub> reference support. This may indicate that Rh particles are located partially on the acidic sites of the supports.

Furthermore, it can also be stated that the number of acidic centres decreased by 40% in the multiple used (6×) rhodium on carbon (8.8 → 5.2 norm. peak area·g<sub>cat</sub><sup>−1</sup>), while this diminution was 72% in the case of rhodium on γ-alumina (39.0 → 11.2 norm. peak area·g<sub>cat</sub><sup>−1</sup>), i.e., remarkably more poison molecules were adsorbed on the acidic sites of the 5% Rh/γ-Al<sub>2</sub>O<sub>3</sub> catalyst than on those of the 5% Rh/C one.

Based on our results, it can be concluded that in the diverse behaviour of 5% Rh/C and 5% Rh/γ-Al<sub>2</sub>O<sub>3</sub> catalysts observed in the acid-free hydrogenation of 1-methylpyrrole (MP), the notably different surface acidity of these catalysts can play a pivotal role.

#### 2.4. Influence of the Amount of Carbon-Supported Rhodium

Since the conversion of MP over 5% Rh/C, at a 0.1 g · g<sup>−1</sup> catalyst/substrate ratio, was complete even after its third reuse at 50 °C (Figure 6b, run 4), the hydrogenation of MP using a lesser amount of catalyst (0.05 g · g<sup>−1</sup> ratio) was also investigated, and its dependence on the number of reusing the catalyst is shown in Figure 9.

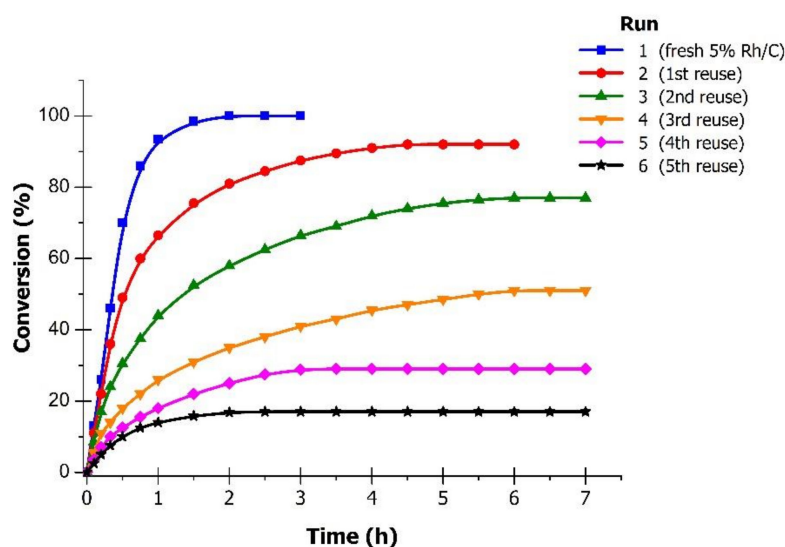


**Figure 9.** Conversion of 1-methylpyrrole (MP) vs. time over 5% Rh/C, at a 0.05 g · g<sup>−1</sup> catalyst/substrate ratio. Conditions: 2.0 g substrate, 50 cm<sup>3</sup> methanol, 50 °C, 10 bar.

As seen, the saturation of pyrrole ring of MP was complete only with the fresh 5% rhodium on carbon (run 1), but this required a longer reaction time (2 h) than applying a 0.1 g · g<sup>−1</sup> catalyst/substrate ratio (0.6 h, Figure 2). Relatively high conversions were obtained (92 and 77%) during the next hydrogenations of MP (runs 2 and 3), but the hydrogen uptake stopped at these levels within 6–7 h. In these cases, the scale of catalyst poisoning by nitrogen [25] had presumably already reached a threshold limit, which resulted in the incomplete conversion of MP. During the next reuse of the catalyst (runs 4–6), intense decreases were observed in the conversion values, which were only 51%, 29%, and 17%, respectively, even after 7 h.

Accordingly, it is favourable to apply a relatively high catalyst/substrate ratio (0.1 g · g<sup>−1</sup>) to achieve full conversion of MP at 50 °C, even after more catalytic runs and using the unregenerated 5% Rh/C catalyst.

To compare the influences of the amount and reuse of 5% Rh/C catalyst on the course of the hydrogenation of MP at 50 °C, the initial rates (*v*<sub>0</sub>) and the final conversions are also depicted in Figure 10.



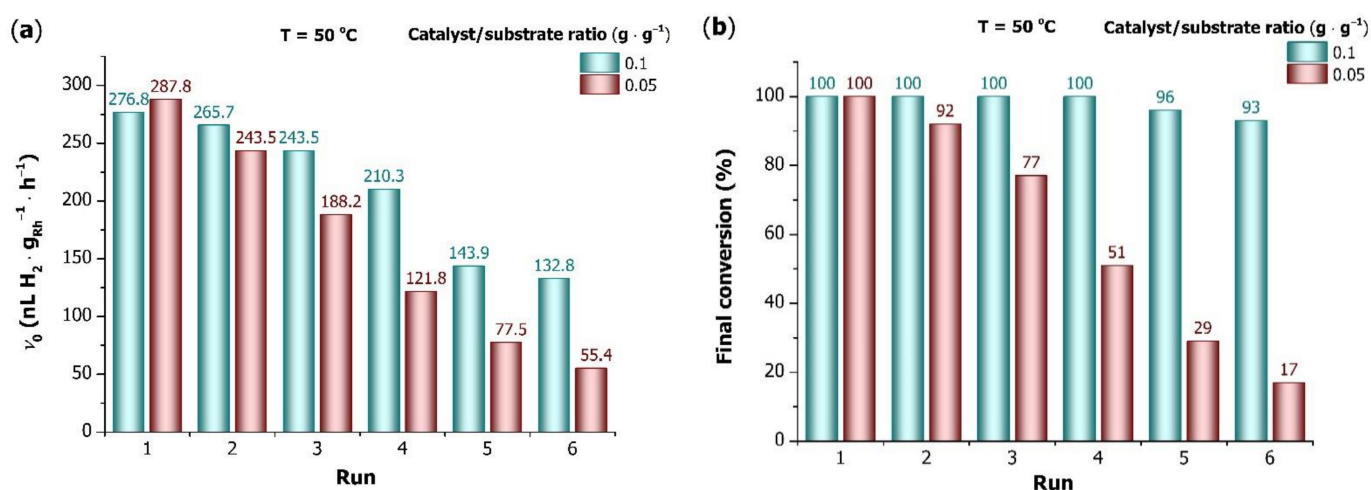


**Figure 10.** Influences of the amount and reuse of the catalyst on the initial rate ( $v_0$ ) (a) and the final conversion (b) in the hydrogenation of 1-methylpyrrole (MP) over 5% Rh/C. Conditions: 2.0 g substrate, 50 cm<sup>3</sup> methanol, 50 °C, 10 bar.

As shown in Figure 10a, a similar diminution of  $v_0$  values was observed by increasing the number of reusing the catalyst ( $276.8 \rightarrow 132.8 \text{ nL H}_2 \cdot \text{g}_{\text{Rh}}^{-1} \cdot \text{h}^{-1}$  and  $287.8 \rightarrow 55.4 \text{ nL H}_2 \cdot \text{g}_{\text{Rh}}^{-1} \cdot \text{h}^{-1}$ , respectively) at both 0.1 and 0.05  $\text{g} \cdot \text{g}^{-1}$  catalyst/substrate ratios. Comparing the final conversions (Figure 10b), more significant differences can be observed. Complete conversion of MP was obtained during almost all runs except the two last ones (96 and 93%, respectively) at a 0.1  $\text{g} \cdot \text{g}^{-1}$  catalyst/substrate ratio, while in the case of a lesser amount of catalyst (0.05  $\text{g} \cdot \text{g}^{-1}$  ratio), a much more appreciable conversion decrease could be noticed after the fifth recycling ( $100 \rightarrow 17\%$ ). This phenomenon alludes to the strong poisoning of rhodium by nitrogen at a lower catalyst/substrate ratio (0.05  $\text{g} \cdot \text{g}^{-1}$ ), even at 50 °C, which becomes more remarkable after several reuses of the 5% Rh/C.

### 2.5. Controlling the Loss of 5% Rh/C

Obviously, the catalyst loss during the recycling operations, i.e., its removal from the reactor, filtration, washing, is inevitable even with the most careful work. A series was performed with 5% Rh/C, where the used catalyst was dried after each hydrogenation reaction, and its weight was measured precisely to properly adjust the substrate loading to keep the catalyst/substrate ratio constant (0.1  $\text{g} \cdot \text{g}^{-1}$ ).

As shown in Figure 11, the course of hydrogenation of MP at 25 °C during the first three catalytic runs was very similar to the reference reaction catalysed by 5% Rh/C (Figure 1a), and the conversion values decreased gradually ( $100 \rightarrow 96 \rightarrow 88\%$ ). In the next runs (4–6), however, much better results were obtained, where the final conversions were around 80% in all cases, and these values were significantly higher than those achieved originally (72, 41, and 35%, respectively). According to the data shown in Table 3, the most notable differences in the conversions were observed when the amount of 5% Rh/C catalyst in a dried form decreased nearly half (0.11–0.07 g) of that in its pristine form (0.20 g).

Based on these results, it is expedient to keep the catalyst/substrate ratio constant during the catalyst recycling, but this requires a drying procedure of the spent catalyst, which could be problematic in practical terms, since varying the catalyst and substrate amounts makes it more difficult to implement the hydrogenation reactions under strict quality-assurance conditions.

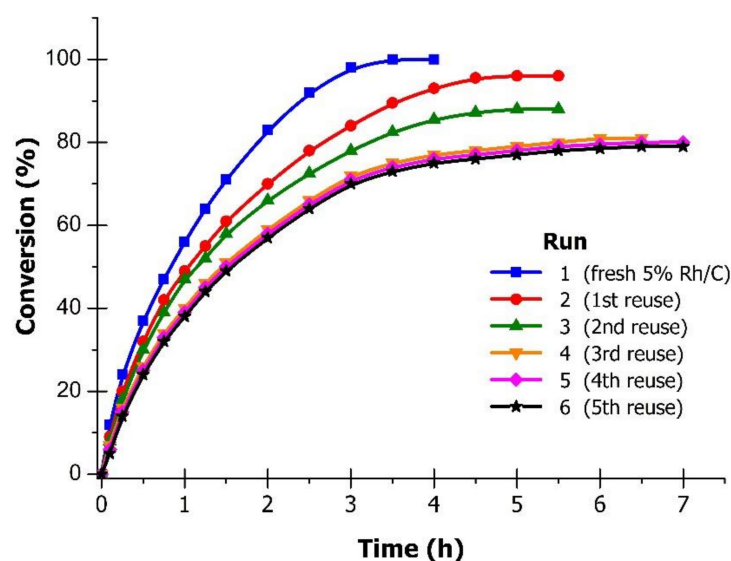


**Figure 11.** Conversion of 1-methylpyrrole (MP) vs. time over 5% Rh/C, at a constant catalyst/substrate ratio ( $0.1 \text{ g} \cdot \text{g}^{-1}$ ). Conditions: 2.0 g substrate,  $50 \text{ cm}^3$  methanol,  $25^\circ \text{C}$ , 10 bar.

**Table 3.** Controlling the catalyst loss during the reuse of 5% Rh/C in the hydrogenation of 1-methylpyrrole (MP).

Run	Reusing the Catalyst	Constant $0.1 \text{ g} \cdot \text{g}^{-1}$ Catalyst/Substrate Ratio		Final Conversion (%)	
		Amount of Catalyst (g)	Amount of Substrate (g)		Reference
1	— (Fresh)	0.20	2.0	100	100
2	1st	0.18	1.8	96	97
3	2nd	0.15	1.5	88	86
4	3rd	0.13	1.3	81	72
5	4th	0.11	1.1	80	41
6	5th	0.07	0.7	79	35

Conditions: 2.0 g substrate,  $50 \text{ cm}^3$  methanol,  $25^\circ \text{C}$ , 10 bar.

## 2.6. Acidic Aftertreatment of Catalysts

Due to the strong basic character of the product (tertiary N atom of 1-methylpyrrolidine), an acidic aftertreatment could be an effective method to avoid the deactivation of catalyst. Since a very drastic decrease was observed in both the activity and the conversion values during the reuse of 5% Rh/C or 5% Rh/ $\gamma\text{-Al}_2\text{O}_3$  at  $25^\circ \text{C}$  (Section 2.1), an acetic acidic handling of the spent catalysts was also examined.

Conversion of MP over 5% rhodium on carbon or  $\gamma$ -alumina treated with 5% acetic acid after each run, at a  $0.1 \text{ g} \cdot \text{g}^{-1}$  catalyst/substrate ratio, depending on the number of reusing the catalyst, in methanol, at  $25^\circ \text{C}$ , is shown in Figure 12.

As seen in Figure 12a, the acidic aftertreatment of the spent 5% Rh/C catalyst resulted in higher conversions of MP in each recycling experiment (runs 2–6) than those achieved in the reference hydrogenations (Figure 1a). The reduction of MP was also complete during the first reuse of the catalyst (run 2), contrary to that obtained without acidic handling (97%). Meanwhile, similar decreases were noted in the conversions in the third and fourth runs as it was observed in those reactions where the 5% rhodium on carbon was applied sans acidic aftertreatment, but better results were achieved (88% and 76%, respectively). Finally, in the fifth and sixth runs, significantly higher conversion values were obtained over the acidic aftertreated catalyst (61 and 47%, respectively) than the untreated one (41 and 35%, respectively).

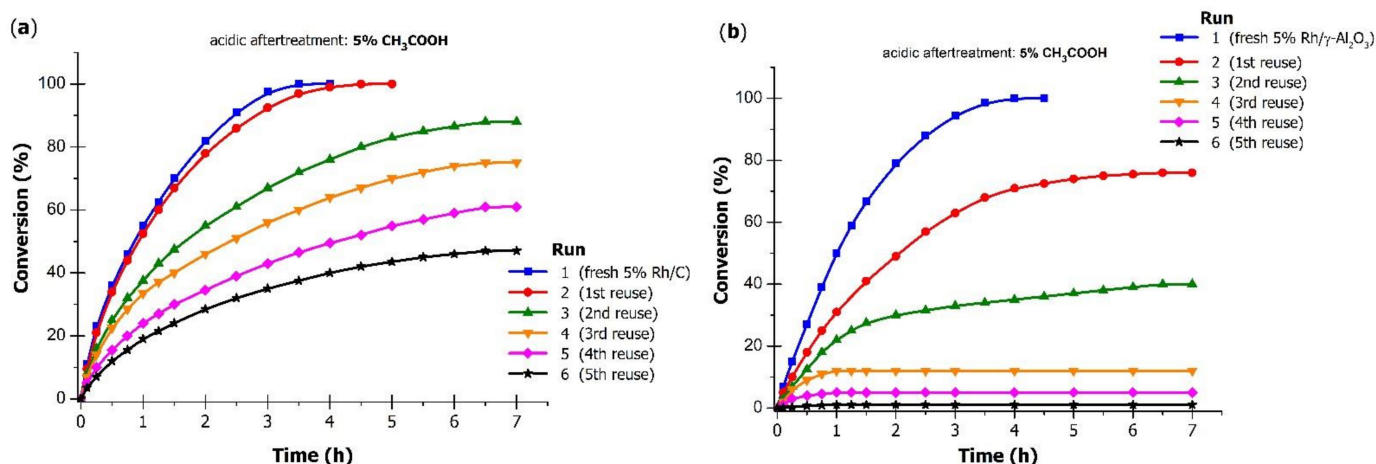


**Figure 12.** Conversion of 1-methylpyrrole (**MP**) vs. time over 5% Rh/C (a) or 5% Rh/γ-Al<sub>2</sub>O<sub>3</sub> (b), applying acidic aftertreatment in each run. Conditions: 2.0 g substrate, 0.2 g catalyst, 50 cm<sup>3</sup> methanol, 25 °C, 10 bar; acidic aftertreatment: 2 × 5 cm<sup>3</sup> 5% acetic acid, then 2 × 10 cm<sup>3</sup> distilled water.

When the 5% Rh/γ-Al<sub>2</sub>O<sub>3</sub> catalyst was aftertreated with 5% acetic acid solution in the hydrogenation of **MP** (Figure 12b), it showed diverse behaviour compared to 5% Rh/C. Although complete conversion was also obtained over the fresh 5% rhodium on γ-alumina (run 1), a significant decrease in the conversion of **MP** was already observed during its first reuse (run 2) when the acidic aftertreatment was applied. Moreover, it was a lower value (76%) than that achieved in the reference reaction (82%) (Figure 1b). In the next recycling experiments (runs 3–6), drastically lower conversions were obtained (40 → 12 → 5 → 1%) after the acidic handling of 5% Rh/γ-Al<sub>2</sub>O<sub>3</sub> than in the reference hydrogenations (43 → 38 → 22 → 14%) (Figure 1b). These results indicate that the γ-alumina support is much more sensitive to acids than the activated-carbon one, and this treatment can cause appreciable changes in its consistency and structure.

Figure 13a–d exhibit the initial rates ( $v_0$ ) and the final conversions to confer the influences of acidic handling and reuse of 5% Rh/C or 5% Rh/γ-Al<sub>2</sub>O<sub>3</sub> catalyst on the course of the hydrogenation of **MP**.

As shown in Figure 13a, a decrease in  $v_0$  values was noticed by increasing the number of reusing the acidic-aftertreated 5% rhodium on carbon catalyst (121.8 → 38.7 nL H<sub>2</sub> · g<sub>Rh</sub><sup>−1</sup> · h<sup>−1</sup>), but they were higher than those observed in the presence of the untreated catalyst (121.8 → 22.1 nL H<sub>2</sub> · g<sub>Rh</sub><sup>−1</sup> · h<sup>−1</sup>). Similarly, the conversions were also diminished (100 → 47%) during the reuse of 5% Rh/C aftertreated with acetic acid (runs 2–6), but these values were significantly higher than those achieved with the untreated catalyst (100 → 35%) (Figure 13b). On the contrary, in the hydrogenations of **MP** over the acidic aftertreated 5% rhodium on γ-alumina, inferior results were obtained compared to those in the reference reductions. Both the initial rates ( $v_0$ ) and the conversion values became much lower (Figure 13c,d), especially after the second reuse of 5% Rh/γ-Al<sub>2</sub>O<sub>3</sub> (runs 4–6). Moreover, in the last catalytic cycle, the full deactivation of the 5% Rh/γ-Al<sub>2</sub>O<sub>3</sub> catalyst aftertreated with acetic acid was detected.

Although better results were obtained applying an acidic-aftertreated 5% Rh/C catalyst, the strong poisoning of rhodium by nitrogen could not be avoided at a 0.1 g · g<sup>−1</sup> catalyst/substrate ratio and room temperature after several reuses of it. In addition, applying 5% Rh/γ-Al<sub>2</sub>O<sub>3</sub> aftertreated with acetic acid showed much weaker activity and stability compared to the untreated catalyst, presumably due to the structural alteration of the γ-alumina support caused by aqueous acid.

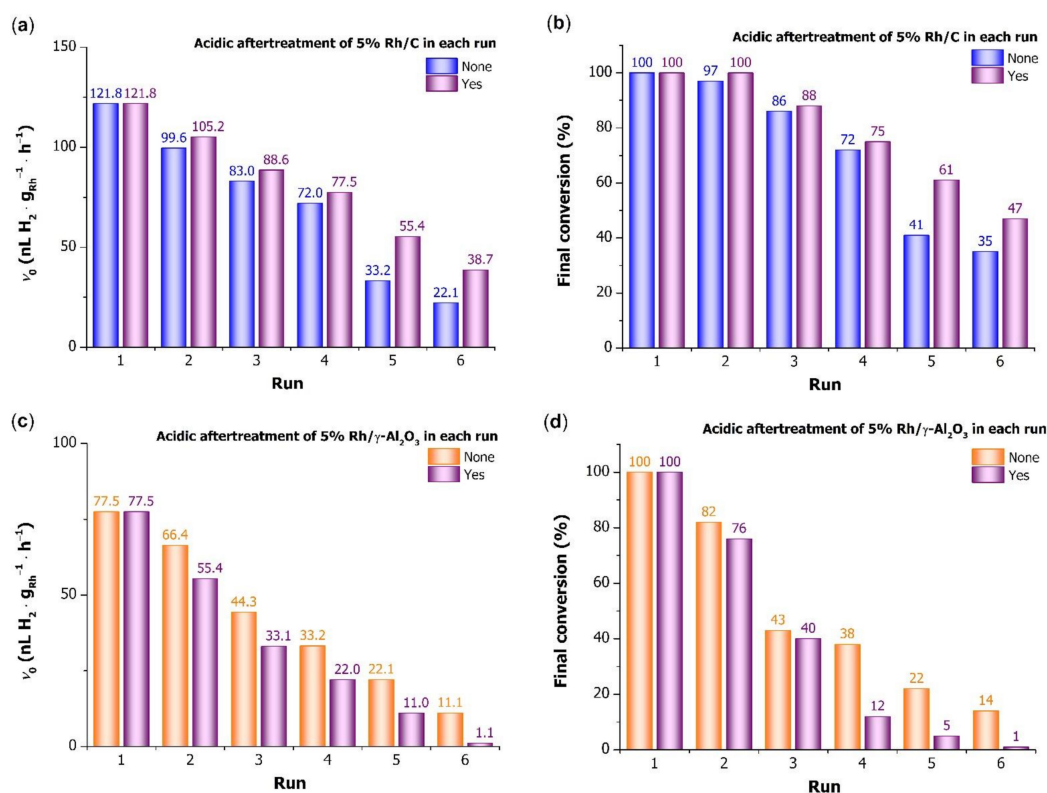


**Figure 13.** Effects of acidic aftertreatment in each run and reuse of the catalyst on the initial rates ( $v_0$ ) and the final conversions in the hydrogenation of 1-methylpyrrole (MP) over 5% Rh/C (a,b) or 5% Rh/ $\gamma$ -Al<sub>2</sub>O<sub>3</sub> (c,d). Conditions: 2.0 g substrate, 0.2 g catalyst, 50 cm<sup>3</sup> methanol, 25 °C, 10 bar; acidic aftertreatment:  $2 \times 5 \text{ cm}^3$  5% acetic acid, then  $2 \times 10 \text{ cm}^3$  distilled water.

### 2.7. Effects of Catalyst Prehydrogenation

Prehydrogenation of the catalyst may serve as a simple method to remove the poisonous, N-containing molecules from the surface of the catalytically active metal (Rh), i.e., hydrogen is able to supplant the formed 1-methylpyrrolidine from the surface of the catalyst and restore the original catalytic activity.

The effects of catalyst prehydrogenation (25 °C, 10 bar, 30 min) in each run and the number of reuses on the conversion of MP over 5% Rh/C or 5% Rh/ $\gamma$ -Al<sub>2</sub>O<sub>3</sub>, at a 0.1 g·g<sup>−1</sup> catalyst/substrate ratio, in methanol, at 10 bar and 25 °C, are depicted in Figure 14.

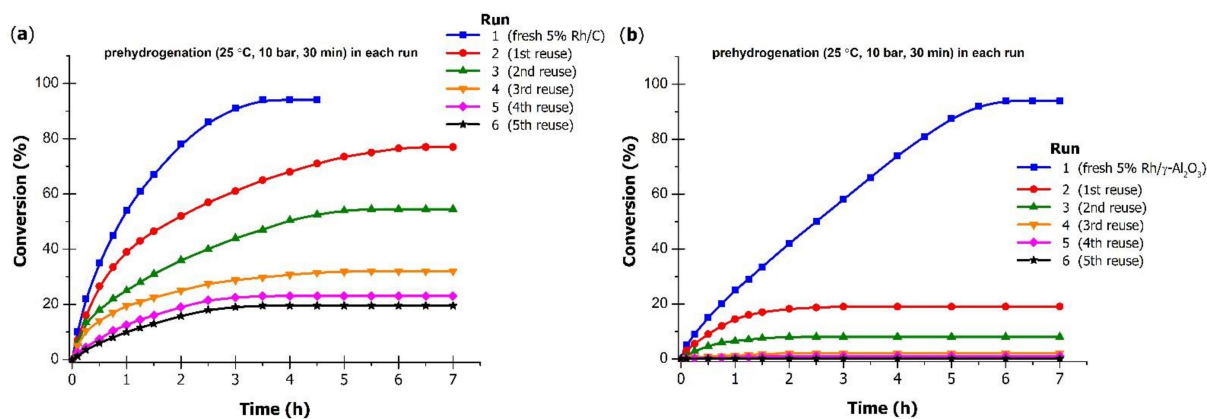


**Figure 14.** Conversion of 1-methylpyrrole (MP) vs. time over prehydrogenated 5% Rh/C (a) or 5% Rh/ $\gamma$ -Al<sub>2</sub>O<sub>3</sub> (b). Conditions: 2.0 g substrate, 0.2 g catalyst, 50 cm<sup>3</sup> methanol, 25 °C, 10 bar; pretreatment: 30 cm<sup>3</sup> methanol, 25 °C, 10 bar, 30 min.

Surprisingly, it was found that the conversion achieved over the prehydrogenated 5% rhodium on carbon (Figure 14a) or 5% rhodium on  $\gamma$ -alumina (Figure 14b) was not complete even using the fresh catalysts (run 1, 94 and 94%, respectively). During the further reuse of 5% Rh/C (runs 2–6), the decline in the conversion values became much more pronounced by increasing the number of reusing the catalyst; specifically, the conversions obtained with the prehydrogenated 5% Rh/C in the three last runs (32  $\rightarrow$  23  $\rightarrow$  19%) were approximately half of those achieved with the untreated catalyst (72  $\rightarrow$  41  $\rightarrow$  35%). A similar trend was also observed in the 5% Rh/ $\gamma$ -Al<sub>2</sub>O<sub>3</sub>-catalysed saturation of pyrrole ring. Moreover, after its second reuse (run 3), practically no conversion of MP was obtained (2  $\rightarrow$  1  $\rightarrow$  0%) even after 7 h, demonstrating that this  $\gamma$ -alumina-supported rhodium catalyst is very sensitive to pretreatment with H<sub>2</sub>, which provokes a strong diminution in its activity. Presumably, the structure of rhodium nanoparticles (e.g., size) could be changed as a result of their interaction with hydrogen.

Figure 15a–d show the initial rates ( $v_0$ ) and the final conversions to compare the influences of prehydrogenation and reuse of 5% Rh/C or 5% Rh/ $\gamma$ -Al<sub>2</sub>O<sub>3</sub> catalysts on the hydrogenation of MP.

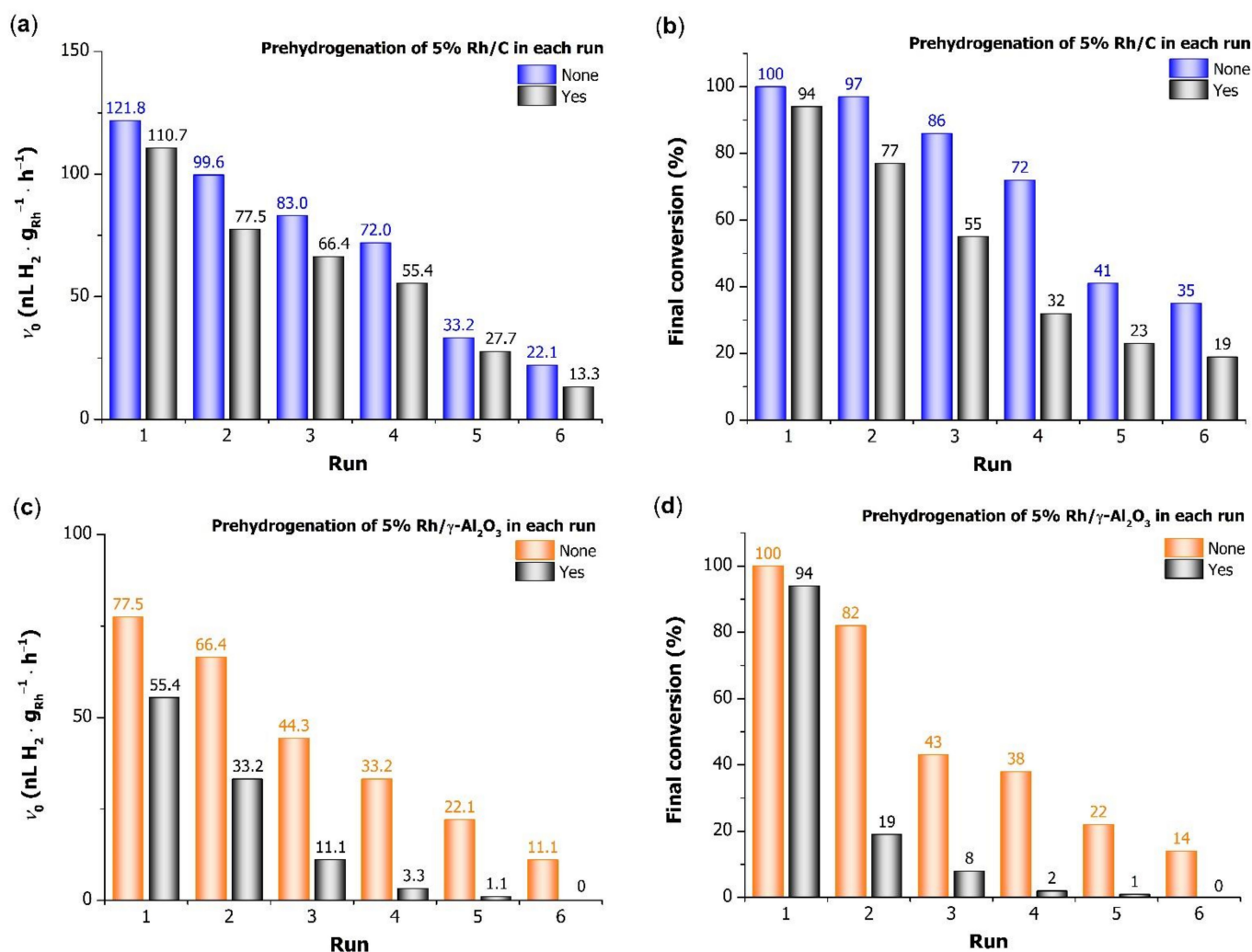


**Figure 15.** Influences of prehydrogenation in each run and reuse of the catalyst on the initial rates ( $v_0$ ) and the final conversions in the reduction of 1-methylpyrrole (MP) over 5% Rh/C (a,b) or 5% Rh/ $\gamma$ -Al<sub>2</sub>O<sub>3</sub> (c,d). Conditions: 2.0 g substrate, 0.2 g catalyst, 50 cm<sup>3</sup> methanol, 25 °C, 10 bar; pretreatment: 30 cm<sup>3</sup> methanol, 25 °C, 10 bar, 30 min.



Similarly to the reference hydrogenations, the  $v_0$  values decreased by increasing the number of reusing the prehydrogenated 5% Rh/C catalyst ( $110.7 \rightarrow 13.3 \text{ nL H}_2 \cdot \text{g}_{\text{Rh}}^{-1} \cdot \text{h}^{-1}$ ), and they were significantly lower than those detected in the presence of the untreated one ( $121.8 \rightarrow 22.1 \text{ nL H}_2 \cdot \text{g}_{\text{Rh}}^{-1} \cdot \text{h}^{-1}$ ) (Figure 15a). Similarly, the conversions were also diminished ( $94 \rightarrow 19\%$ ) during the reuse of 5% rhodium on carbon pretreated with  $\text{H}_2$  (runs 1–6), and these values were also appreciably lower than those obtained with the untreated catalyst ( $100 \rightarrow 35\%$ ) (Figure 15b). More drastic alterations were found in the hydrogenations of **MP** over the prehydrogenated 5% rhodium on  $\gamma$ -alumina, where both the initial rates ( $v_0$ ) and the conversion values became much worse (Figure 15c,d) even after its first use (runs 2–6). Moreover, in the last catalytic run, a complete loss of activity of the 5% Rh/ $\gamma$ - $\text{Al}_2\text{O}_3$  catalyst pretreated with hydrogen was observed (zero conversion and  $v_0$  values).

Based on our results, it can be stated that poisoning of these supported rhodium catalysts could not be avoided by their prehydrogenation; moreover, their activities were significantly diminished.

To clarify the observed differences between untreated and prehydrogenated Rh catalysts on different supports (activated C,  $\gamma$ - $\text{Al}_2\text{O}_3$ ) in fresh or used ( $6\times$ ) form, their morphologies were revealed by transmission electron microscopy (Figure 16), and their dispersions were characterised by  $\text{O}_2$ - and  $\text{H}_2$ -titration measurements.

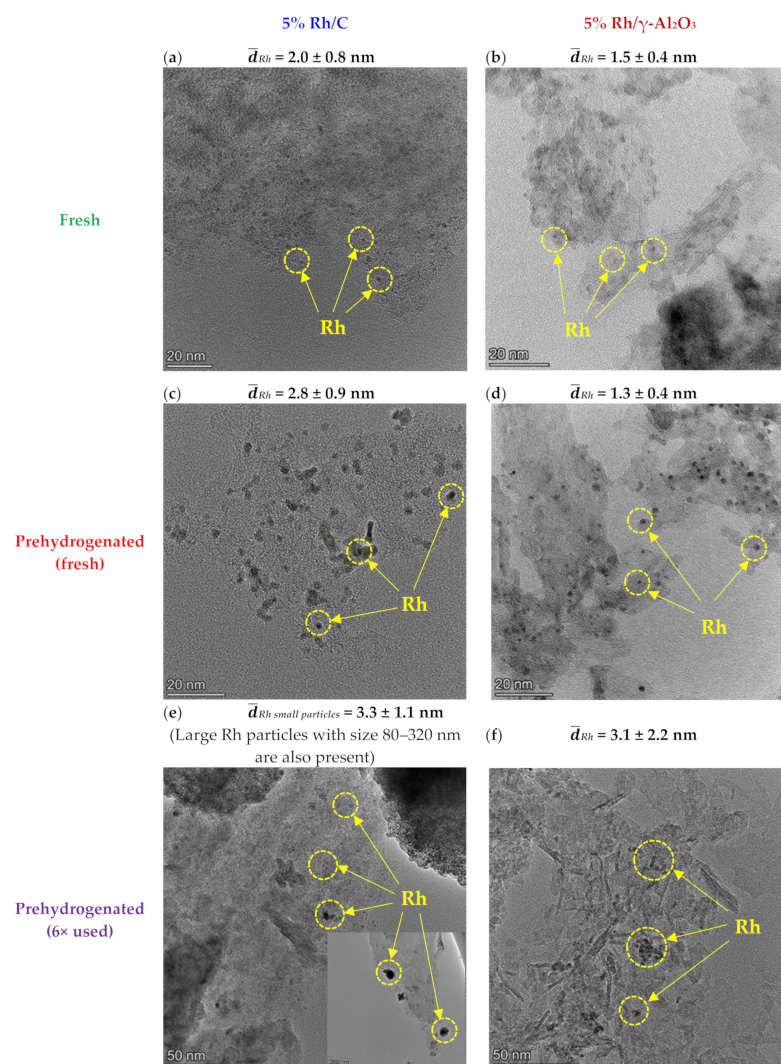


**Figure 16.** TEM images and the average Rh particle sizes of 5% Rh/C and 5% Rh/ $\gamma$ - $\text{Al}_2\text{O}_3$  catalysts in fresh (a,b), prehydrogenated (fresh) (c,d), and prehydrogenated ( $6\times$  used) (e,f) forms.

As shown in Figure 16a,b, both fresh catalysts contained small and homodisperse Rh particles (several groups of them are highlighted by yellow circles), and their average size was  $\sim 2.0$  nm in the 5% Rh/C catalyst, while it was  $\sim 1.5$  nm in the 5% Rh/ $\gamma$ -Al<sub>2</sub>O<sub>3</sub> one. After prehydrogenation of the fresh catalysts, in case of the carbon-supported rhodium, the size of the primary particles of rhodium was slightly increased to  $\sim 2.8$  nm, and their aggregates could be observed (Figure 16c). The rhodium dispersion was more stable on the  $\gamma$ -alumina support under the prehydrogenation, contrary to its much lower specific surface area, but likely due to the higher surface density of acidic sites and a stronger metal–support interaction. The mean particle diameter ( $\sim 1.3$  nm) and the size distribution remained practically the same (Figure 16d). Thus, the lower activity of the prehydrogenated 5% Rh/Al<sub>2</sub>O<sub>3</sub> catalysts cannot be explained by any sintering of rhodium. Presumably, a stronger adsorption interaction between the product molecules (MPD) and the prehydrogenated metal rhodium particles and, thus, an enhanced blocking of catalytically active sites, can occur. On the other hand, reduction in the Rh surface on the carbon support due to the ca. 40% particle size increase could cause a loss of activity compared to the reference measurements sans prehydrogenation. Thus, the prehydrogenation did not enhance the poisoning of the rhodium surface on the activated-carbon support as much as on the alumina support.

When the prehydrogenated catalysts were repeatedly used ( $6\times$ ), their morphologies were significantly changed (Figure 16e,f), in that heterodisperse Rh particles could be recognised in these supported catalysts. In the case of 5% Rh/C (Figure 16e), in addition to the smaller particles below 7 nm in size (sometimes in several particle aggregations) with  $3.3 \pm 1.1$  nm mean diameter, several very large rhodium particles (80–320 nm) were also observed. In the 5% Rh/ $\gamma$ -Al<sub>2</sub>O<sub>3</sub> catalyst, the mean particle size also increased (to  $3.1 \pm 2.2$  nm), and the particles formed loose groups (Figure 16f), but no very large particles were detected.

The accessible Rh surface was probed by O<sub>2</sub>- and H<sub>2</sub>-titration. A relatively high-temperature but short pretreatment (350 °C) of the catalysts was necessary to remove the contaminants from their surface. This could cause sintering of the Rh nanoparticles, but lower-temperature pretreatments resulted in lower dispersion values. Unfortunately, on the 5% Rh/C sample an increase in the mean size was observed from  $2.0 \pm 0.8$  nm (fresh sample, Figure 16a) to  $2.3 \pm 0.6$  nm, with the appearance of large particles as well, and the consumed O<sub>2</sub> and H<sub>2</sub> were lower than after H<sub>2</sub> pretreatment at 120 °C—a much lower temperature. Thus, the carbon-supported samples could not be measured reliably, without modification by the pretreatment with H<sub>2</sub>- or O<sub>2</sub>-titration. However, in the case of 5% Rh/ $\gamma$ -Al<sub>2</sub>O<sub>3</sub> after the pretreatment up to 350 °C and H<sub>2</sub>- and O<sub>2</sub>-titration, the mean Rh particle diameter did not change significantly, it was  $1.3 \pm 0.4$  nm as compared to the  $1.5 \pm 0.4$  nm of the fresh sample (Figure 16b), as measured by TEM. Thus, the accessible Rh surface could be compared in the different states of the alumina-supported catalyst by H<sub>2</sub>- and O<sub>2</sub>-titration. After prehydrogenating the fresh 5% Rh/ $\gamma$ -Al<sub>2</sub>O<sub>3</sub> catalyst, its dispersion remained unchanged (0.38), but a very large decrease was observed in it (to 0.04) when this rhodium catalyst was used six times and prehydrogenated in each run (Table 4).

**Table 4.** Dispersion of the 5%  $\gamma$ -alumina-supported Rh catalyst in an untreated (fresh) or prehydrogenated form.

Entry	Form of 5% Rh/ $\gamma$ -Al <sub>2</sub> O <sub>3</sub>	Dispersion (–) <sup>a</sup>
1	Untreated (fresh)	0.38
2	Prehydrogenated <sup>b</sup> (fresh)	0.38
3	Prehydrogenated <sup>b</sup> ( $6\times$ used)	0.04

<sup>a</sup> Determined by O<sub>2</sub>- and H<sub>2</sub>-titration measurements. <sup>b</sup> Prehydrogenation: 25 °C, 10 bar, 30 min.

Based on these results, in the case of 5% Rh/ $\gamma$ -Al<sub>2</sub>O<sub>3</sub>, the deactivating effect of prehydrogenation cannot be explained by a decrease in the accessible Rh surface (due to neither sintering nor to blocking by any contaminant). In the case of 5% Rh/C, the sintering

observed due to prehydrogenation can explain the larger observed deactivation compared to the fresh catalyst. After multiple uses, more significant Rh sintering was detected on both the alumina and activated-carbon supports, but the poisoning of the active sites played the dominant role in the drastic activity loss.

### 3. Materials and Methods

#### 3.1. Materials

1-Methylpyrrole (99%) was supplied by Merck-Schuchardt (Hohenbrunn, Germany), while methanol (p. a.) was purchased from Merck (Darmstadt, Germany).

The 5% Rh/ $\gamma$ -Al<sub>2</sub>O<sub>3</sub> catalyst (Degussa G214 R/D) was received from Aldrich (Steinheim, Germany), whilst 5% Rh/C was prepared according to our procedure described in [18], using a Carbopal P3-type activated carbon (Donau Carbon, Frankfurt, Germany) as a catalyst support.  $\gamma$ -Aluminium oxide nanopowder (99+%) was supplied by Alfa Aesar—part of Thermo Fisher Scientific (Kandel, Germany).

#### 3.2. Hydrogenations

The hydrogenation reactions were carried out in a 250 cm<sup>3</sup> stainless steel autoclave (Technoclave, Budapest, Hungary) equipped with a magnetic stirrer (stirring speed: 1100 rpm) and an electric heating system, at 10 bar and 25–50 °C. Typically, the reactor containing **MP** (2.0 g), 5% Rh/C or 5% Rh/ $\gamma$ -Al<sub>2</sub>O<sub>3</sub> catalyst (0.2 g), and methanol (50 cm<sup>3</sup>) was flushed with nitrogen and hydrogen, and then charged with hydrogen to the specified pressure and heated up to the given temperature, if necessary. After finishing the hydrogen uptake, the catalyst was filtered off and a sample was taken from the filtrate. The sample was analysed by GC–MS, and the final conversion was determined by using the gas-chromatographic data. The actual conversion values were calculated from the decrease in hydrogen pressure, as defined by Equations (1) and (2):

$$\text{Conversion (\%)} = \frac{\Delta n_{H_2}}{n_{\text{total } H_2}} \times 100 \quad (1)$$

$$\Delta n_{H_2} = \frac{\Delta p_{H_2} \cdot V}{R \cdot T} \quad (2)$$

where  $\Delta n_{H_2}$  is the amount of hydrogen consumed in the reaction (mol),  $n_{\text{total } H_2}$  is the amount of hydrogen required to complete the reaction (mol),  $\Delta p_{H_2}$  is the measured decrease in pressure (Pa),  $V$  is the free volume of the autoclave ( $2 \times 10^{-4}$  m<sup>3</sup>),  $R$  is the universal gas constant ( $8.314 \text{ J} \cdot \text{mol}^{-1} \cdot \text{K}^{-1}$ ), and  $T$  is the actual reaction temperature (K).

The initial rate ( $v_0$ ) was determined from the conversion curves according to Equation (3):

$$v_0 = \frac{\Delta V_{H_2}}{m_{Rh} \cdot \Delta t} \quad (3)$$

where  $v_0$  is the initial rate extrapolated to  $t = 0$ ,  $\Delta V_{H_2}$  is the volume of hydrogen at 10% conversion (nL),  $\Delta t$  is the time for 10% conversion (h), and  $m_{Rh}$  is the amount of rhodium (g).

1-Methylpyrrolidine (**MPD**), when the conversion was complete, was prepared in the same way as described in [19]. The MS data of the starting material and the product were as follows: **MP**  $m/z$  (rel%) 81(100), 55(15), 53(26), 42(24), 39(23); **MPD**  $m/z$  (rel%) 85(55), 84(97), 57(90), 42(100), 32(8). These analytical results are consistent with the literature data [58].

#### 3.3. Catalyst Recycling

After filtering the spent catalyst, it was washed with distilled water ( $2 \times 5 \text{ cm}^3$ ) and collected carefully to be stored for the next reaction, in wet form. No regenerative processes were applied prior to its reuse.

When an acidic treatment of the used catalyst was implemented, the procedure was as follows: The spent catalyst was filtered and suspended in 5% acetic acid ( $2 \times 5 \text{ cm}^3$ ), and then washed with distilled water ( $2 \times 10 \text{ cm}^3$ ) to pH = 7. Finally, it was also collected carefully to be stored for the next reaction, in the same wet form.

### 3.4. Catalyst Pretreatment

The prehydrogenation of 5% Rh/C or 5% Rh/ $\gamma$ -Al<sub>2</sub>O<sub>3</sub> was carried out in the absence of a substrate (MP), in methanol, at 10 bar and 25 °C for 30 min. After this pretreatment, MP was added to the reaction mixture at 25 °C, and its hydrogenation was performed at 25 or 50 °C.

### 3.5. Correction of Catalyst Loss

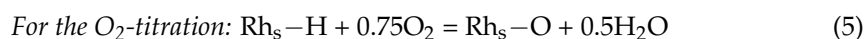
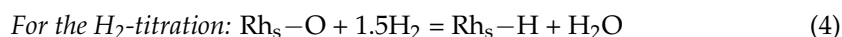
In this series, the catalyst/substrate ratio was kept at 0.1 g · g<sup>−1</sup> in each reaction carried out over 5% Rh/C. The used catalyst was filtered and dried at 80 °C after finishing the H<sub>2</sub> uptake, and the amount of substrate (MP) was calculated based on the weight of the dried catalyst. The hydrogenations were performed without any treatments, at 25 °C.

### 3.6. Catalyst Characterisation

Specific surface areas of the catalysts (5% Rh/C, 5% Rh/ $\gamma$ -Al<sub>2</sub>O<sub>3</sub>) and the supports (activated carbon,  $\gamma$ -alumina) were determined by measuring nitrogen adsorption–desorption isotherms using a NOVA<sup>®</sup> 2000e (Quantachrome, Boynton Beach, FL, USA) automated volumetric nitrogen gas adsorption instrument at −196 °C. Preparation of samples (degassing in vacuum) was performed at 110 °C for 24 h. The apparent surface area (*S*<sub>BET</sub>) was calculated with the Brunauer–Emmett–Teller (BET) model [59].

Surface acidity of the catalysts and their supports was characterised by temperature-programmed ammonia desorption (NH<sub>3</sub>-TPD) measurements using a micromeritics<sup>®</sup> AutoChem<sup>®</sup> II 2920 (Automated Catalyst Characterization System, Micromeritics Instrument Corp., Norcross, GA, USA) equipped with a quadrupole mass spectrometer (QMS, ThermoStar, Pfeiffer Vacuum). It should be noted that the pure carbon support was from the same batch as that used for the preparation of the Rh/C sample, while although the pure Al<sub>2</sub>O<sub>3</sub> was also  $\gamma$ -type like the support of the commercial 5% Rh/ $\gamma$ -Al<sub>2</sub>O<sub>3</sub>, they were not the same. Each sample (50 mg) was pretreated by heating up to 350 °C (10 °C/min) to remove the hydrocarbons and water adsorbed due to ambient contaminations from its surface, and after 10 min they were cooled down to 40–50 °C in helium flow. Then adsorption of ammonia was carried out in helium containing 10% NH<sub>3</sub> for 15 min, followed by flushing with helium (50 cm<sup>3</sup>/min) at the same temperature for 30 min to remove the weakly bound NH<sub>3</sub>. NH<sub>3</sub>-TPD (also in He) was performed afterwards by heating to 500 °C at 20 °C/min, and the ion current of *m/e* = 17 (for NH<sub>3</sub>) and *m/e* = 18 (for H<sub>2</sub>O) was recorded by QMS. For NH<sub>3</sub> concentration, the *m/e* = 17 signal was corrected by subtracting the contribution of the *m/e* = 17 fragment ion of H<sub>2</sub>O. The amount of desorbed NH<sub>3</sub> was characterised by integration of the corrected *m/e* = 17 ion current versus the time of TPD.

Dispersion of rhodium was determined by O<sub>2</sub>- and H<sub>2</sub>-titration of the H<sub>2</sub>- and O<sub>2</sub>-covered catalyst samples, respectively, using the same AutoChem<sup>®</sup> II 2920, but with its thermal conductivity detector (TCD). The catalyst samples (30 mg) were first pretreated by heating up to 350 °C at a rate of 10 °C/min in helium flow to clean their surfaces of ambient contaminations. After cooling to 25 °C, they were contacted with 10% O<sub>2</sub>/He flow for 15 min to saturate the surface with adsorbed oxygen (Rh<sub>s</sub>–O), which was titrated with H<sub>2</sub> using 10% H<sub>2</sub>/Ar pulses in Ar flow. Then, the H-saturated surface (Rh<sub>s</sub>–H) was titrated with O<sub>2</sub> (10% O<sub>2</sub>/He pulses in He flow) in the same way, and it was followed by another titration with H<sub>2</sub>. The H<sub>2</sub>O formed during titrations was trapped at about −80 °C from the effluent gas mixture before the TCD detector. From the consumed H<sub>2</sub> and O<sub>2</sub>, the amounts of the surface Rh atoms (Rh<sub>s</sub>) were calculated using the stoichiometry of Equations (4) and (5), respectively:



The dispersion values (number of Rh<sub>s</sub>/number of total Rh) derived from the O<sub>2</sub>-titration and the subsequent (second) H<sub>2</sub>-titration were almost equal (the differences were below 5%), except in the case of the multiple used catalyst, where it was much larger.

Morphology of the catalysts drop-dried from an ethanol suspension onto a carbon-coated copper grid was investigated by transmission electron microscopy (TEM), using a FEI Titan Themis 200 kV Cs-corrected TEM with an HRTEM resolution of 0.09 nm. The average size of the Rh particles was determined by measuring at least 300 metal particles from randomly selected non-aggregated areas of each sample, using ImageJ software.

### 3.7. Analysis

The components of the reaction mixtures were analysed and identified by GC–MS. The analyses were carried out with an Agilent 7890A GC-system (7683 autosampler and 7683B injector) connected to an Agilent 5975C mass spectrometer using a Restek Rxi®-5Sil MS capillary column (15 m × 0.25 mm ID, 0.25 µm film). The temperature program was as follows: 45 °C (1 min) to 300 °C at 50 °C/min; hold for 1 min.

## 4. Conclusions

Poisoning phenomena caused by nitrogen and the reuse of a heterogeneous, carbon- or  $\gamma$ -alumina-supported rhodium catalyst were investigated in the hydrogenation of 1-methylpyrrole (**MP**), as a model compound, in a non-acidic liquid phase (methanol). Reusing the spent, unregenerated 5% Rh/C or 5% Rh/ $\gamma$ -Al<sub>2</sub>O<sub>3</sub>, the activity of catalyst and the conversion of **MP** were strongly dependent on the number of reuses, the supports, the temperature, the amount of catalyst, and its pre- or aftertreatment.

These various supported rhodium catalysts already provided high activity in their fresh form at 25 °C, but they showed a different poison tolerance, the 5% Rh/ $\gamma$ -Al<sub>2</sub>O<sub>3</sub> catalyst had an appreciably lower one than the 5% Rh/C catalyst. In addition, increasing the temperature to 50 °C resulted in higher catalytic activity and final conversions over 5% rhodium on carbon in all of its reuses, but when using 5% rhodium on  $\gamma$ -alumina the raised temperature (50 or 80 °C) induced a significant conversion diminution and intensified the catalyst's deactivation during its multiple reuses (6×). From the NH<sub>3</sub>–TPD measurements, notable differences in the surface acidity of these catalysts were evidenced, which must play a role in their diverse behaviour in this acid-free hydrogenation. This surface analytical method revealed that more poison molecules (1-methylpyrrolidine, **MPD**) could be adsorbed on the more acidic fresh catalyst and the used  $\gamma$ -alumina-supported catalyst than on the activated-carbon-supported one, both on the fresh and the used 5% Rh/C catalysts.

To obtain the complete conversion of **MP** over 5% Rh/C even after more catalytic runs, and without regeneration of the catalyst, a relatively high catalyst/substrate ratio (0.1 g · g<sup>−1</sup>) was applied, because in the presence of a lesser amount of catalyst (0.05 g · g<sup>−1</sup> ratio), significant decreases in conversion and activity were observed even at 50 °C. This was due to the strong poisoning of rhodium caused by the basic nitrogen of the product (**MPD**). However, reusing the spent and unregenerated 5% rhodium on carbon above a certain catalyst/substrate ratio can be an alternative method for Rh-catalysed, heterogeneous catalytic hydrogenation processes applied in the fine chemical industry.

Although an acidic aftertreatment of the used catalysts resulted in better conversions applying 5% Rh/C at a 0.1 g · g<sup>−1</sup> catalyst/substrate ratio and 25 °C, the deactivation caused by nitrogen could not be avoided. Moreover, in the case of 5% Rh/ $\gamma$ -Al<sub>2</sub>O<sub>3</sub>, a drastic conversion diminution was detected after its acidic handling, indicating that the  $\gamma$ -alumina support is much more sensitive to acids than the activated-carbon support, and that this treatment can cause notable alterations in its consistency and structure.

Using the prehydrogenated catalysts, surprisingly, no complete conversions were obtained over either 5% Rh/C or 5% Rh/ $\gamma$ -Al<sub>2</sub>O<sub>3</sub>, even using them in fresh form, and their catalytic activities, especially that of 5% Rh/ $\gamma$ -Al<sub>2</sub>O<sub>3</sub>, were drastically reduced after multiple reuses. This unexpected catalytic behaviour of 5% Rh/C and 5% Rh/ $\gamma$ -Al<sub>2</sub>O<sub>3</sub> was clarified by TEM measurements, as well as O<sub>2</sub>- and H<sub>2</sub>-titration (catalyst dispersion). Due to the prehydrogenation of the fresh catalysts, no changes in Rh particle size and dispersion were detected in the 5% Rh/ $\gamma$ -Al<sub>2</sub>O<sub>3</sub> catalyst, while slight sintering of Rh was



observed in 5% Rh/C. On the other hand, it was revealed that the morphology of the rhodium particles on both alumina and carbon was changed after their multiple reuses, and a heterodisperse structure of the aggregated metal particles with somewhat increased size was formed. In addition, the 5% Rh/C catalyst contained very large particles as well. However, the dominant factor in the declining activity in the repeated runs must be the poisoning of both supported Rh catalysts.

As a final conclusion, the optimal reaction conditions that would allow a high yield of this product (MPD) to be achieved with multiple uses of the catalyst, without regeneration, are as follows. Using 5% carbon-supported rhodium, a catalyst/substrate ratio no less than  $0.1 \text{ g} \cdot \text{g}^{-1}$ , a temperature of  $50^\circ\text{C}$ , and applying a treatment of the catalyst with acetic acid after each run. Meanwhile, the prehydrogenation degrades the catalytic performance of rhodium, and the BET area of the catalysts and the stronger acidity of the  $\text{Al}_2\text{O}_3$  are not as critical as the sizes of the Rh particles.

Further investigations to clarify the poisoning mechanisms of other nitrogen-containing heterocycles (pyridines) over precious metal catalysts (palladium, rhodium, ruthenium) are in progress.

**Author Contributions:** Conceptualisation, L.H. and A.B.; methodology, L.H. and A.B.; formal analysis, K.L. (Krisztina László), G.S. and A.B.; investigation, T.T.T.N. and K.L. (Krisztina Lévy); writing—original draft preparation, L.H.; writing—review and editing, L.H., G.S. and A.B.; visualisation, L.H., G.S. and A.B.; supervision, L.H.; project administration, L.H.; funding acquisition, L.H. All authors have read and agreed to the published version of the manuscript.

**Funding:** The research reported in this paper and carried out at BME was supported by the NRDI Fund (TKP2020 NC, Grant No. BME-NC), based on the charter of bolster issued by the NRDI Office under the auspices of the Ministry for Innovation and Technology. The Themis microscope was purchased within the framework of a Hungarian national project VEKOP-2.3.3-15-2016-00002.

**Data Availability Statement:** All the relevant data are included in this published article.

**Acknowledgments:** The authors thank Tibor Novák and Miklós Nyerges (Servier Research Institute, Hungary) for providing GC–MS measurements.

**Conflicts of Interest:** The authors declare no conflict of interest.

## References

1. Hegedűs, L.; Szőke-Molnár, K.; Sajó, I.E.; Srankó, D.F.; Schay, Z. Poisoning and Reuse of Supported Precious Metal Catalysts in the Hydrogenation of *N*-heterocycles Part I: Ruthenium-Catalysed Hydrogenation of 1-Methylpyrrole. *Catal. Lett.* **2018**, *148*, 1939–1950. [\[CrossRef\]](#)
2. Hegedus, L.L.; McCabe, R.W. *Catalyst Poisoning*; Marcel Dekker: New York, NY, USA, 1984.
3. Forzatti, P.; Lietti, L. Catalyst deactivation. *Catal. Today* **1999**, *52*, 165–181. [\[CrossRef\]](#)
4. Bartholomew, C.H. Mechanisms of catalyst deactivation. *Appl. Catal. A Gen.* **2001**, *212*, 17–60. [\[CrossRef\]](#)
5. Besson, M.; Gallezot, P. Deactivation of metal catalysts in liquid phase organic reactions. *Catal. Today* **2003**, *81*, 547–559. [\[CrossRef\]](#)
6. Moulijn, J.A.; van Diepen, A.E.; Kapteijn, F. Deactivation and Regeneration. In *Handbook of Heterogeneous Catalysis*; Ertl, G., Knözinger, H., Schüth, F., Weitkamp, J., Eds.; Wiley-VCH Verlag: Weinheim, Germany, 2008; pp. 1829–1845.
7. Guisnet, M.; Ribeiro, F.R. Deactivation and regeneration of solid catalysts. In *Deactivation and Regeneration of Zeolite Catalysts*; Guisnet, M., Ribeiro, F.R., Eds.; Catalytic Science Series—Volume 9; Imperial College Press: London, UK, 2011; pp. 3–18.
8. Argyle, M.D.; Bartholomew, C.H. Heterogeneous Catalyst Deactivation and Regeneration: A Review. *Catalysts* **2015**, *5*, 145–269. [\[CrossRef\]](#)
9. Lange, J.-P. Renewable Feedstocks: The Problem of Catalyst Deactivation and its Mitigation. *Angew. Chem. Int. Ed.* **2015**, *54*, 13186–13197. [\[CrossRef\]](#)
10. Hamilton, T.S.; Adams, R. Reduction of pyridine hydrochloride and pyridonium salts by means of hydrogen and platinum-oxide platinum black. XVIII. *J. Am. Chem. Soc.* **1928**, *50*, 2260–2263. [\[CrossRef\]](#)
11. Maxted, E.B.; Walker, A.G. Studies in the detoxication of catalyst poisons. Part VII. The self-poisoning effect in the hydrogenation of pyridine. *J. Chem. Soc.* **1948**, 1093–1097. [\[CrossRef\]](#)
12. Maxted, E.B. The Poisoning of Metallic Catalysts. *Adv. Catal.* **1951**, *3*, 129–178.
13. Devereux, J.M.; Payne, K.R.; Peeling, E.R.A. Catalytic hydrogenation. Part I. The hydrogenation of unsaturated amines over platinum oxide. *J. Chem. Soc.* **1957**, 2845–2851. [\[CrossRef\]](#)

14. Maxted, E.B.; Briggs, M.S. The catalytic toxicity of nitrogen compounds. Part I. Toxicity of ammonia and of amines. *J. Chem. Soc.* **1957**, 3844–3847. [\[CrossRef\]](#)
15. Freifelder, M. *Practical Catalytic Hydrogenation*; John Wiley: New York, NY, USA, 1971.
16. Petró, J. Catalyst poisons, catalyst poisoning. In *Contact Catalysis*; Szabó, Z.G., Kalló, D., Eds.; Elsevier: Amsterdam, The Netherlands, 1976; Volume 2, pp. 65–75.
17. Hegedűs, L. Katalizátorok mérgeződése, katalizátorméreg típusú vegyületek hidrogénezése. *Magy. Kém. Folyóirat* **2007**, *113*, 139–144.
18. Xi, Y.; Huang, L.; Cheng, H. Mechanisms of Pyrrole Hydrogenation on Ru(0001) and Hydrogen Molybdenum Bronze Surfaces. *J. Phys. Chem. C* **2015**, *119*, 22477–22485. [\[CrossRef\]](#)
19. He, T.; Liu, L.; Wu, G.; Chen, P. Covalent triazine framework-supported palladium nanoparticles for catalytic hydrogenation of *N*-heterocycles. *J. Mater. Chem. A* **2015**, *3*, 16235–16241. [\[CrossRef\]](#)
20. Kim, T.W.; Oh, J.; Suh, Y.-W. Hydrogenation of 2-benzylpyridine over alumina-supported Ru catalysts: Use of Ru<sub>3</sub>(CO)<sub>12</sub> as a Ru precursor. *Appl. Catal. A Gen.* **2017**, *547*, 183–190. [\[CrossRef\]](#)
21. Moghaddam, A.A.; Krewer, U. Poisoning of Ammonia Synthesis Catalyst Considering Off-Design Feed Compositions. *Catalysts* **2020**, *10*, 1225. [\[CrossRef\]](#)
22. Choi, J.; Cho, A.; Cho, J.H.; Kim, B.M. Bimetallic PdRh-Fe<sub>3</sub>O<sub>4</sub> nanoparticle-catalyzed highly selective quinoline hydrogenation using ammonia borane. *Appl. Catal. A Gen.* **2022**, *642*, 118709. [\[CrossRef\]](#)
23. Hegedűs, L.; Máthé, T.; Tungler, A. Hydrogenation of pyrrole derivatives I. Hydrogenations over palladium. *Appl. Catal. A Gen.* **1996**, *143*, 309–316. [\[CrossRef\]](#)
24. Hegedűs, L.; Máthé, T.; Tungler, A. Hydrogenation of pyrrole derivatives. II. Hydrogenations over supported noble metal catalysts. *Appl. Catal. A Gen.* **1996**, *147*, 407–414. [\[CrossRef\]](#)
25. Hegedűs, L.; Máthé, T.; Tungler, A. Hydrogenation of pyrrole derivatives. Part IV. Hydrogenation of 1-methylpyrrole. *Appl. Catal. A Gen.* **1997**, *152*, 143–151. [\[CrossRef\]](#)
26. Hegedűs, L.; Máthé, T.; Tungler, A. Hydrogenation of pyrrole derivatives Part III. Hydrogenation of methyl 1-methyl-2-pyrroleacetate. *Appl. Catal. A Gen.* **1997**, *153*, 133–139. [\[CrossRef\]](#)
27. Nikiforov, T.; Stanchev, S.; Milenkov, B.; Dimitrov, V. Asymmetric synthesis of 1-methyl-2-(2-hydroxyethyl)pyrrolidine. *Heterocycles* **1986**, *24*, 1825–1829. [\[CrossRef\]](#)
28. Fournier, A.M.; Brown, R.A.; Farnaby, W.; Miyatake-Ondozabal, H.; Clayden, J. Synthesis of (–)-(S,S)-clemastine by Invertive N → C Aryl Migration in a Lithiated Carbamate. *Org. Lett.* **2010**, *12*, 2222–2225. [\[CrossRef\]](#) [\[PubMed\]](#)
29. Lee, S.Y.; Jung, J.W.; Kim, T.-H.; Kim, H.-D. Asymmetric synthesis of H<sub>1</sub> receptor antagonist (R,R)-clemastine. *Arch. Pharm. Res.* **2015**, *38*, 2131–2136. [\[CrossRef\]](#) [\[PubMed\]](#)
30. Leete, E. 1-Methylpyrrolidine-2-acetic Acid, a Plausible Intermediate in the Biosynthesis of Cocaine. *Heterocycles* **1989**, *28*, 481–487. [\[CrossRef\]](#)
31. Hegedűs, L.; Máthé, T. Hydrogenation of pyrrole derivatives Part V. Poisoning effect of nitrogen on precious metal on carbon catalysts. *Appl. Catal. A Gen.* **2002**, *226*, 319–322. [\[CrossRef\]](#)
32. Tungler, A.; Hegedűs, L.; Háda, V.; Máthé, T.; Szepesy, L. Diastereoselective Heterogeneous Catalytic Hydrogenation of Chiral Aromatic *N*-Heterocyclic Compounds. *Chem. Ind. Cat. Org. React.* **2001**, *82*, 425–437.
33. Háda, V.; Tungler, A.; Szepesy, L. Diastereoselective heterogeneous catalytic hydrogenation of *N*-heterocycles: Part II. Hydrogenation of pyrroles. *Appl. Catal. A Gen.* **2001**, *210*, 165–171. [\[CrossRef\]](#)
34. Eblagon, K.M.; Tam, K.; Tsang, S.C.E. Comparison of catalytic performance of supported ruthenium and rhodium for hydrogenation of 9-ethylcarbazole for hydrogen storage applications. *Energy Environ. Sci.* **2012**, *5*, 8621–8630. [\[CrossRef\]](#)
35. Song, S.; Fung Kin Yuen, V.; Di, L.; Sun, Q.; Zhou, K.; Yan, N. Integrating Biomass into the Organonitrogen Chemical Supply Chain: Production of Pyrrole and D-Proline from Furfural. *Angew. Chem. Int. Ed.* **2020**, *59*, 19846–19850. [\[CrossRef\]](#)
36. Overberger, C.G.; Palmer, L.C.; Marks, B.S.; Byrd, N.R. Azo Compounds. Biradical Sources. The Synthesis of Some 1,1-Disubstituted Hydrazines. *J. Am. Chem. Soc.* **1955**, *77*, 4100–4104. [\[CrossRef\]](#)
37. Adams, R.; Miyano, S.; Nair, M.D. Synthesis of Substituted Pyrrolidines and Pyrrolizidines. *J. Am. Chem. Soc.* **1961**, *83*, 3323–3327. [\[CrossRef\]](#)
38. Ortiz, C.; Greenhouse, R. The total synthesis of (+)-isoretronecanol from pyrrole. *Tetrahedron Lett.* **1985**, *26*, 2831–2832. [\[CrossRef\]](#)
39. Jiang, C.; Frontier, A.J. Stereoselective Synthesis of Pyrrolidine Derivatives via Reduction of Substituted Pyrroles. *Org. Lett.* **2007**, *9*, 4939–4942. [\[CrossRef\]](#)
40. Kotthaus, A.F.; Ballaschk, F.; Stakaj, V.; Mohr, F.; Kirsch, S.F. Synthesis and Resolution of a Chiral Diamine: 2,2'-(Propane-2,2-diyl)dipyrrolidine. *Synthesis* **2017**, *49*, 3107–3111.
41. Cincinelli, R.; Beretta, G.; Dallavalle, S. Total synthesis of tetracyclic kynurenic acid analogues isolated from chestnut honey. *Tetrahedron Lett.* **2018**, *59*, 163–166. [\[CrossRef\]](#)
42. Journot, G.; Neier, R.; Gualandi, A. Hydrogenation of Calix [4]pyrrole: From the Formation to the Synthesis of Calix [4]pyrrolidine. *Eur. J. Org. Chem.* **2021**, *2021*, 4444–4464. [\[CrossRef\]](#)
43. Huang, W.; Kuhn, J.N.; Tsung, C.-K.; Zhang, Y.; Habas, S.E.; Yang, P.; Somorjai, G.A. Dendrimer Templated Synthesis of One Nanometer Rh and Pt Particles Supported on Mesoporous Silica: Catalytic Activity for Ethylene and Pyrrole Hydrogenation. *Nano Lett.* **2008**, *8*, 2027–2034. [\[CrossRef\]](#)

44. Kliewer, C.J.; Bieri, M.; Somorjai, G.A. Pyrrole Hydrogenation over Rh(111) and Pt(111) Single-Crystal Surfaces and Hydrogenation Promotion Mediated by 1-Methylpyrrole: A Kinetic and Sum-Frequency Generation Vibrational Spectroscopy Study. *J. Phys. Chem. C* **2008**, *112*, 11373–11378. [[CrossRef](#)]
45. Hagelüken, C. Precious metals process catalysts—Material flows and recycling. *Chim. Oggi/Chem. Today* **2006**, *24*, 14–17.
46. Hagelüken, C. Recycling of spent catalysts containing precious metals. In *Handbook of Heterogeneous Catalysis*; Ertl, G., Knözinger, H., Schüth, F., Weitkamp, J., Eds.; Wiley-VCH Verlag: Weinheim, Germany, 2008; pp. 1846–1863.
47. Axon, S.A.; Casci, J.L. Recycling of spent catalysts containing base metals. In *Handbook of Heterogeneous Catalysis*; Ertl, G., Knözinger, H., Schüth, F., Weitkamp, J., Eds.; Wiley-VCH Verlag: Weinheim, Germany, 2008; pp. 1863–1871.
48. Trimm, D.L. The regeneration or disposal of deactivated heterogeneous catalysts. *Appl. Catal. A Gen.* **2001**, *212*, 153–160. [[CrossRef](#)]
49. Grumett, P. Precious Metal Recovery from Spent Catalysts. *Platinum Metals Rev.* **2003**, *47*, 163–166.
50. Marafi, M.; Stanislaus, A. Options and processes for spent catalyst handling and utilization. *J. Hazard. Mater.* **2003**, *B101*, 123–132. [[CrossRef](#)]
51. Jackson, S.D. Processes occurring during deactivation and regeneration of metal and metal oxide catalysts. *Chem. Eng. J.* **2006**, *120*, 119–125.
52. Dufresne, P. Hydroprocessing catalysts regeneration and recycling. *Appl. Catal. A Gen.* **2007**, *322*, 67–75. [[CrossRef](#)]
53. Al-Sheeha, H.; Marafi, M.; Raghavan, V.; Rana, M.S. Recycling and Recovery Routes for Spent Hydroprocessing Catalyst Waste. *Ind. Eng. Chem. Res.* **2013**, *52*, 12794–12801. [[CrossRef](#)]
54. Molnár, Á.; Papp, A. Catalyst recycling—A survey of recent progress and current status. *Coord. Chem. Rev.* **2017**, *349*, 1–65. [[CrossRef](#)]
55. Miceli, M.; Frontera, P.; Macario, A.; Malara, A. Recovery/Reuse of Heterogeneous Supported Spent Catalysts. *Catalysts* **2021**, *11*, 591. [[CrossRef](#)]
56. EudraLex—Volume 4, Good Manufacturing Practice (GMP) Guidelines. Available online: [https://ec.europa.eu/health/medicinal-products/eudralex/eudralex-volume-4\\_hu](https://ec.europa.eu/health/medicinal-products/eudralex/eudralex-volume-4_hu) (accessed on 5 May 2022).
57. Busca, G. The surface of transitional aluminas: A critical review. *Catal. Today* **2014**, *226*, 2–13. [[CrossRef](#)]
58. *NIST Chemistry WebBook, NIST Standard Reference Database Number 69*; Linstrom, P.J.; Mallard, W.G. (Eds.) National Institute of Standards and Technology: Gaithersburg, MD, USA, 2017. [[CrossRef](#)]
59. Brunauer, S.; Emmett, P.; Teller, E. Adsorption of Gases in Multimolecular Layers. *J. Am. Chem. Soc.* **1938**, *60*, 309–319. [[CrossRef](#)]